EUROPEAN ORGANIZATION FOR NUCLEAR RESEARCH

NP Internal Report 75-2
26 February 1975

SUMMARY OF THE RESULTS OF THE EXPERIMENT ON CHARGED PARTICLE PRODUCTION AT MEDIUM ANGLES PERFORMED AT THE CERN ISR (R202)

E. Albini, P. Capiluppi, A.M. Rossi and G. Vannini

Istituto di Fisica dell'Università and INFN, Sezione di Bologna, Bologna, Italy

A. Bussière

CERN, Geneva, Switzerland, and DPHN/HE, Saclay, France

D. D'Alessandro and G. Giacomelli

Istituto di Fisica dell'Università di Padova and INFN, Sezione di Padova, Padova, Italy

G E N E V A

1975

This is a "pictorial" summary of the results obtained in an experiment on single inclusive reactions performed by the Bologna-CERN Collaboration at the CERN-ISR using the medium-angle spectrometer in the I2 intersection region (experiment R202).

The reactions studied were

$$\begin{aligned} p + p &\to \pi^{\pm} + \text{anything} , \\ &\to K^{\pm} + \text{anything} , \\ &\to p^{\pm} + \text{anything} . \end{aligned}$$

For details, we refer to the publications[1-7], in particular to the last three. In this note, only the particle ratios represent new unpublished results. The errors quoted for the ratios are statistical only, except for the values of Tables 4 and 8, where the errors include also the systematic uncertainties and uncertainties arising from the corrections.

The following figures and tables are included:

i) Invariant cross-sections $Ed^3\sigma/d^3p$
   - versus x : Figs. 1.1 and 1.2,
   - versus y_{lab} : Figs. 2.1 and 2.2,
   - versus p_t : Figs. 3.1 to 3.3,
   - versus p_t^2 : Figs. 4.1 and 4.2,
   - versus m_ℓ : Fig. 5,
   - versus p : Fig. 6,
   - versus $\sqrt{s}$: Figs. 7.1 to 7.8.

ii) Average transverse momentum $\langle p_t \rangle$
   - versus x : Fig. 8,
   - versus y_{lab} : Fig. 8,
   - versus p_{lab} : Fig. 9.

iii) Average multiplicity of charged particles
   - versus s : Fig. 10.1.

iv) Particle composition
   - versus x : Fig. 10.2b,
   - versus y_{lab} : Fig. 10.2a,
   - versus p_t : Figs. 10.2.

v) Ratios between invariant cross-sections
   - versus x : Figs. 11.1 to 11.3, Tables 1 and 2,
   - versus y_{lab} : Figs. 12.1 and 12.2, Tables 3 and 4,
   - versus p_t : Figs. 13.1 to 13.5, Tables 5 to 8.

We would like to acknowledge the collaboration of O. Ferrari, who drew most of the figures and contributed to all the stages of the experiment.

* * *

REFERENCES

1) A. Bertin, P. Capiluppi, A. Cristallini, M. D'Agostino-Bruno, R.J. Ellis, G. Giacomelli, C. Maroni, F. Mercatali, A.M. Rossi and G. Vannini, Negative particle production at the CERN-ISR, Phys. Letters 38 B, 260 (1972).

2) A. Bertin, P. Capiluppi, M. D'Agostino-Bruno, R.J. Ellis, G. Giacomelli, A.M. Rossi, G. Vannini, A. Bussière and R.T. Poe, Charged particle production ratios at the CERN-ISR for a transverse momentum of 0.4 GeV/c, Phys. Letters 41 B, 201 (1972).

3) A. Bertin, P. Capiluppi, M. D'Agostino-Bruno, R.J. Ellis, G. Giacomelli, A.M. Rossi, G. Vannini, A. Bussière and R.T. Poe, Charged particle production at the CERN-ISR as a function of transverse momentum, Phys. Letters 42 B, 493 (1972).

4) M. Antinucci, A. Bertin, P. Capiluppi, M. D'Agostino-Bruno, G. Giacomelli, A.M. Rossi, G. Vannini and A. Bussière, Multiplicities of charged particles up to ISR energies, Nuovo Cimento Letters 6, 121 (1973).

5) P. Capiluppi, G. Giacomelli, A.M. Rossi, G. Vannini and A. Bussière, Transverse momentum dependence in p-p inclusive reactions at very high energies, Nuclear Phys. B70, 1 (1974).

6) P. Capiluppi, G. Giacomelli, A.M. Rossi, G. Vannini, A. Bertin, A. Bussière and R.J. Ellis, Charged particle production in p-p inclusive reactions at very high energies, Nuclear Phys. B79, 189 (1974).

7) A.M. Rossi, G. Vannini, A. Bussière, E. Albini, D. D'Alessandro and G. Giacomelli, Experimental study of the energy dependence in p-p inclusive reactions, Nuclear Phys. B84, 269 (1975).

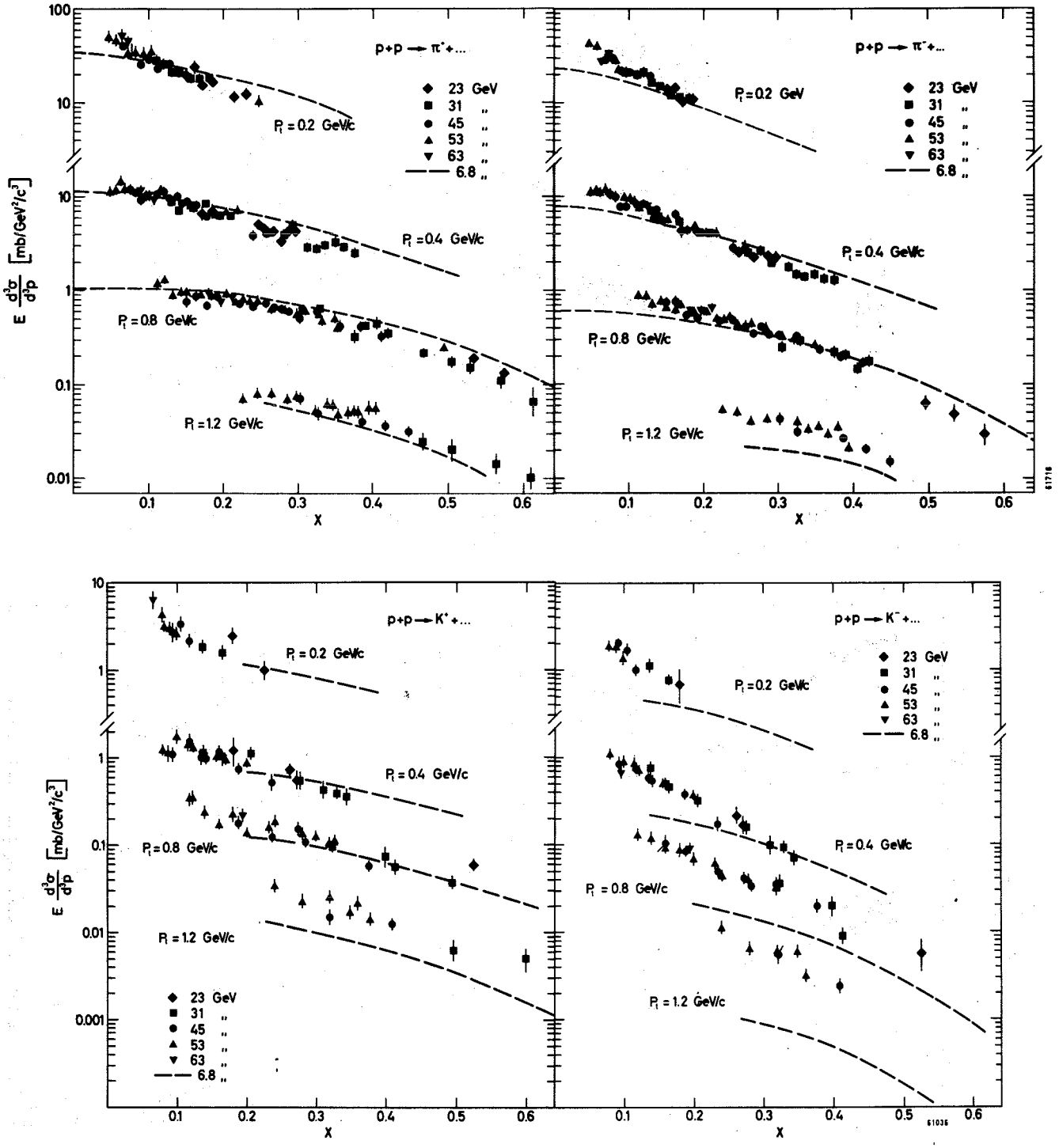

Fig. 1.1 The invariant cross-sections for π^+, π^-, K^+, and K^- production versus x at p_t = 0.2, 0.4, 0.8, and 1.2 GeV/c (Ref. 6)

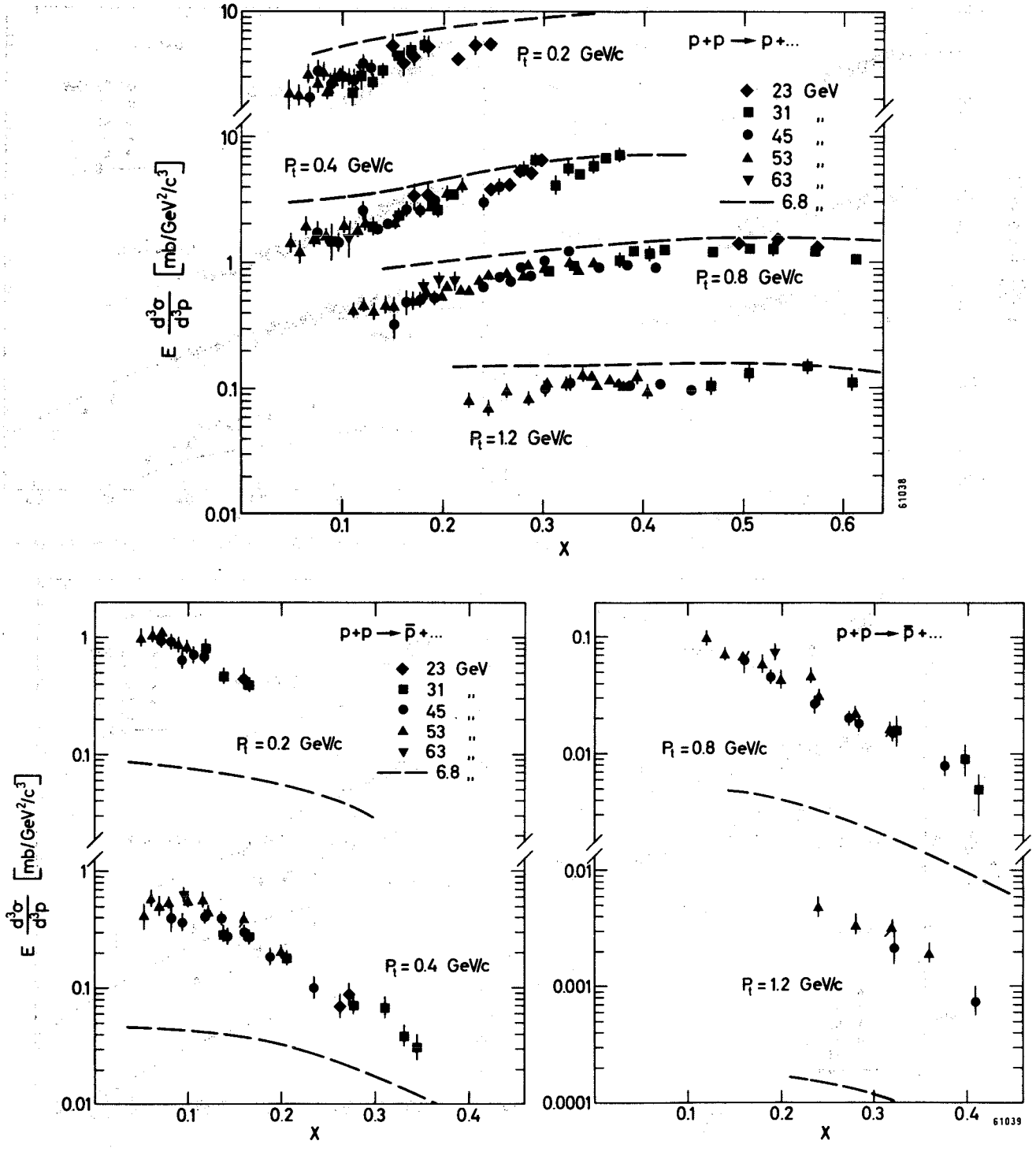

Fig. 1.2 The invariant cross-sections for p and $\bar{p}$ production versus x at p_t = 0.2, 0.4, 0.8, and 1.2 GeV/c (Ref. 6)

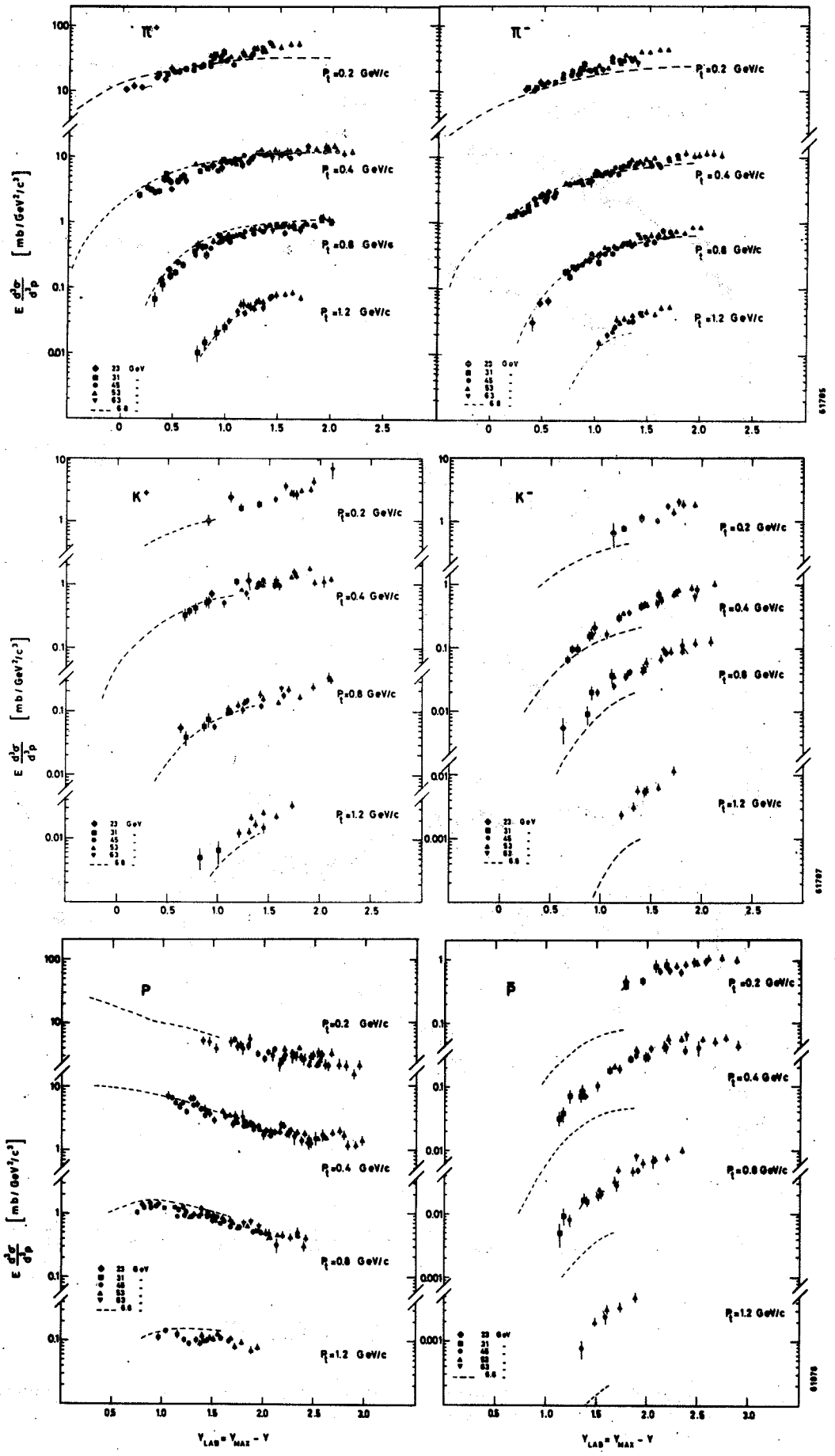

Fig. 2.1 The invariant cross-sections for π^+, π^-, K^+, K^-, p, and $\bar{p}$ production versus y_{lab} at p_t = 0.2, 0.4, 0.8, and 1.2 GeV/c (Ref. 6)

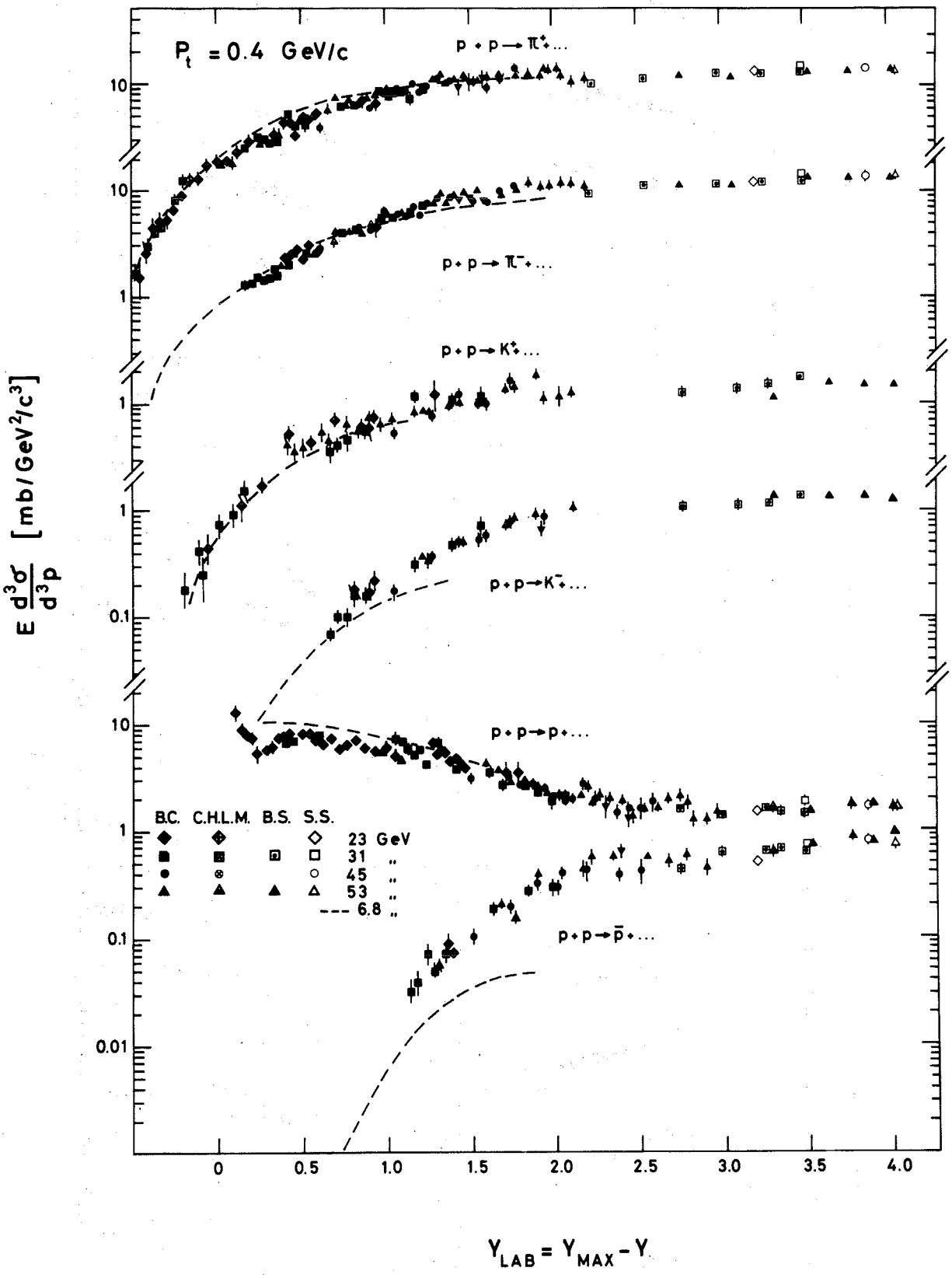

Fig. 2.2 The invariant cross-sections for π^+, π^-, K^+, K^-, p, and $\bar{p}$ production versus y_{lab} at p_t = 0.4 GeV/c (Ref. 6)

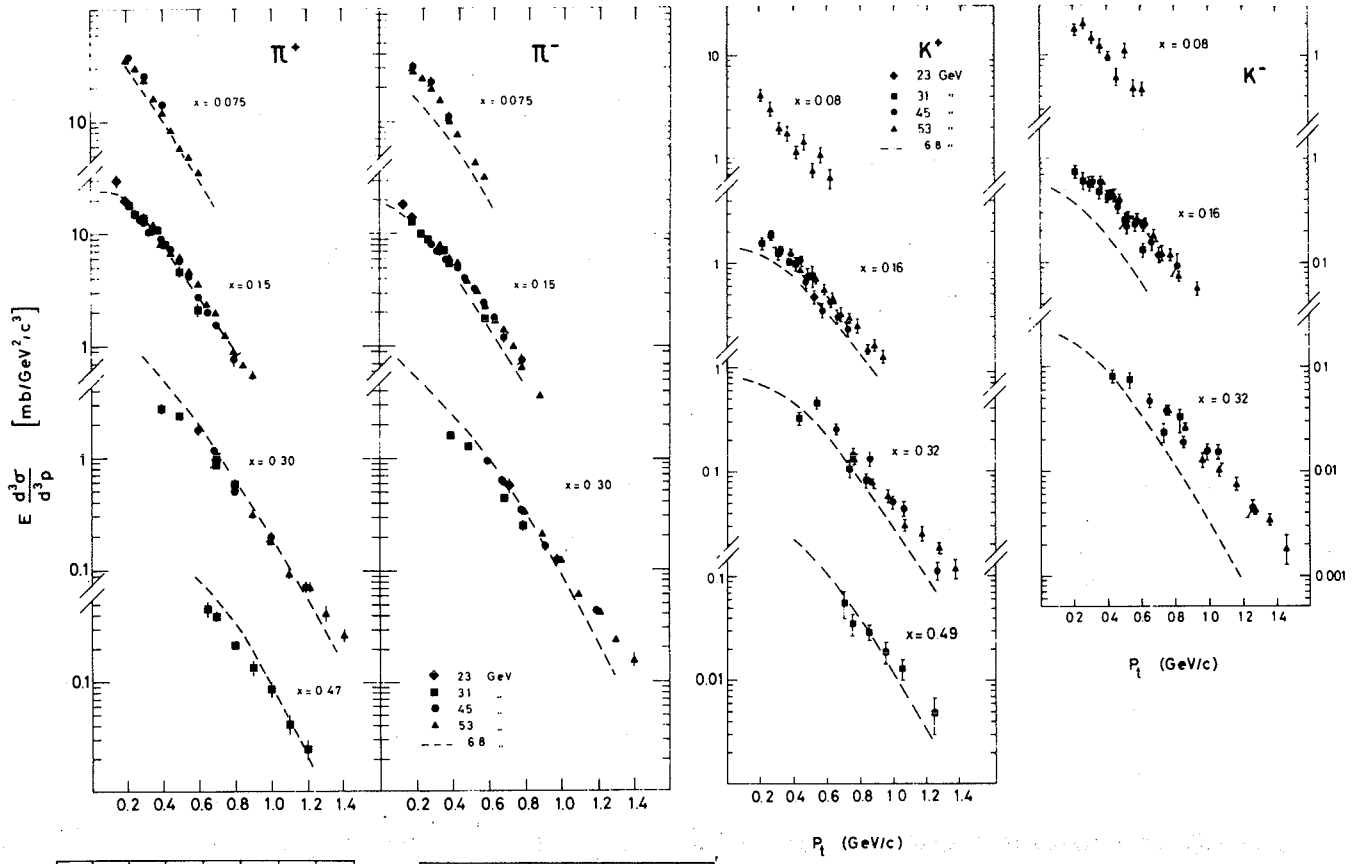

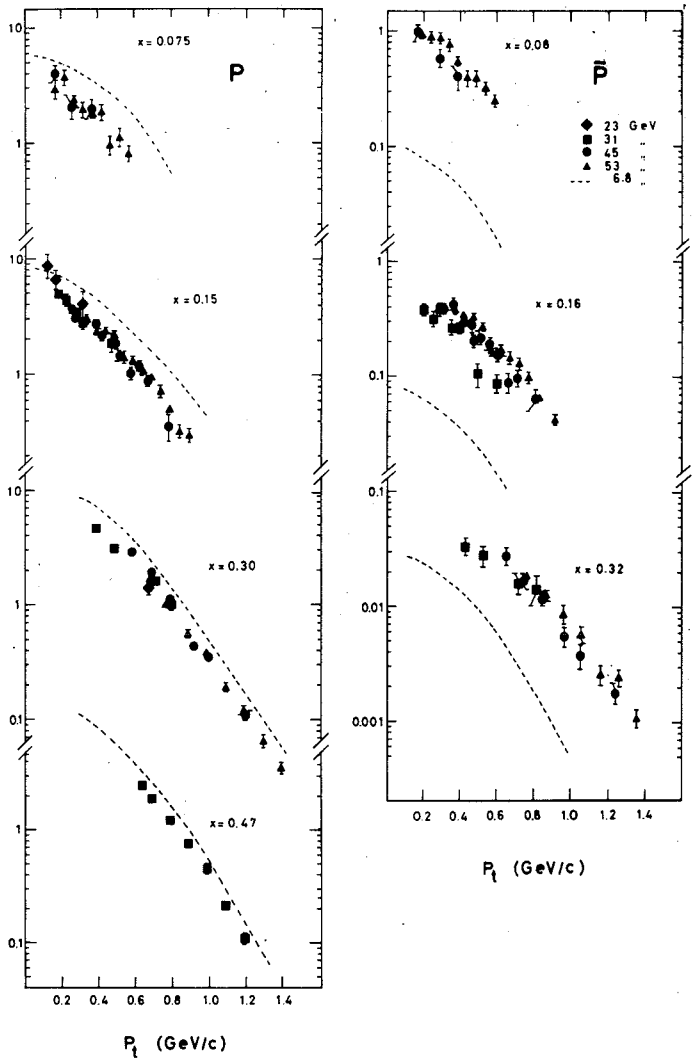

Fig. 3.1
The invariant cross-sections for π^+, π^-, K^+, K^-, p, and $\bar{p}$ production versus p_t at x ≃ 0.08, 0.15, 0.30, and 0.49 (Ref. 5)

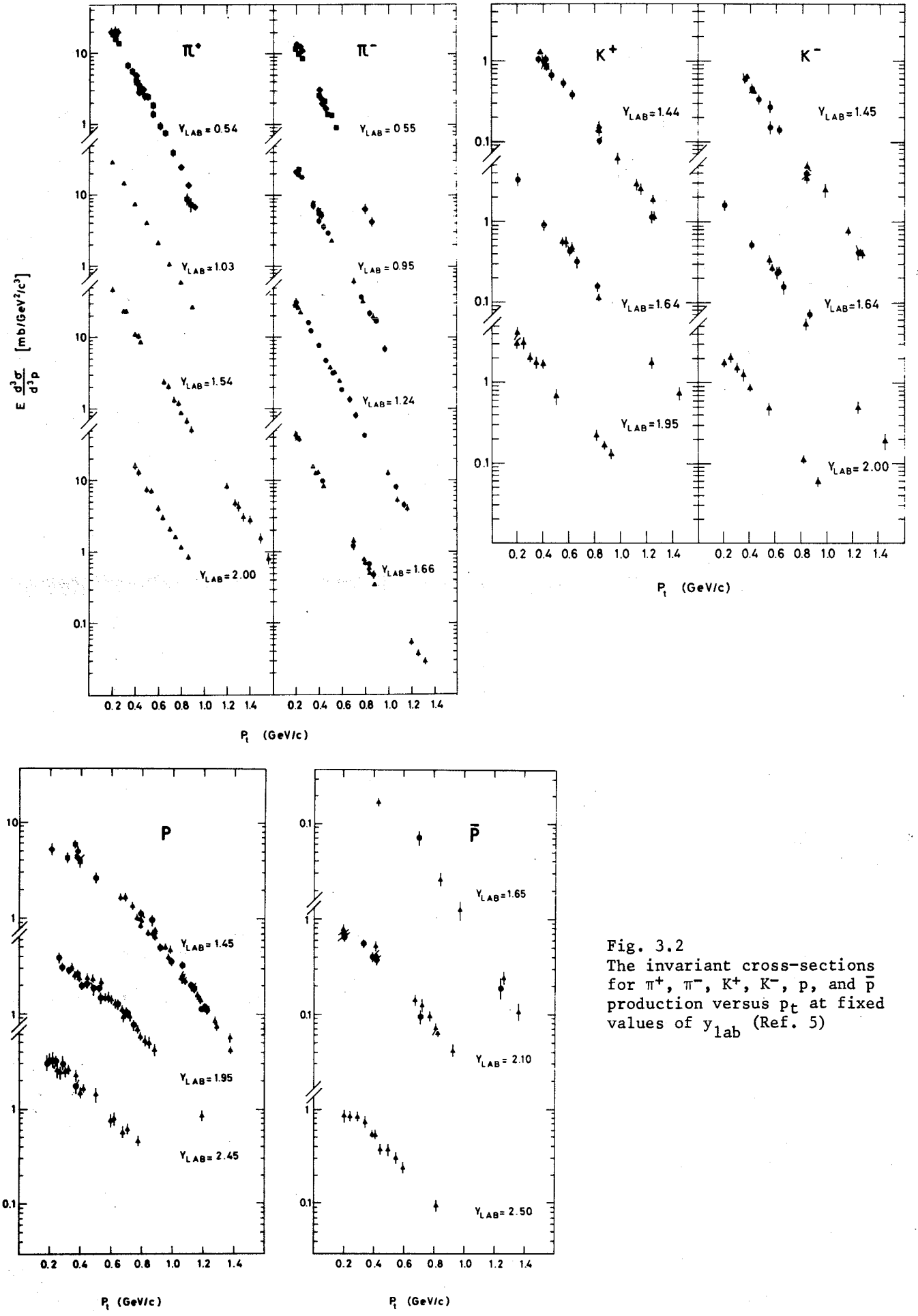

Fig. 3.2
The invariant cross-sections for π^+, π^-, K^+, K^-, p, and $\bar{p}$ production versus p_t at fixed values of y_{lab} (Ref. 5)

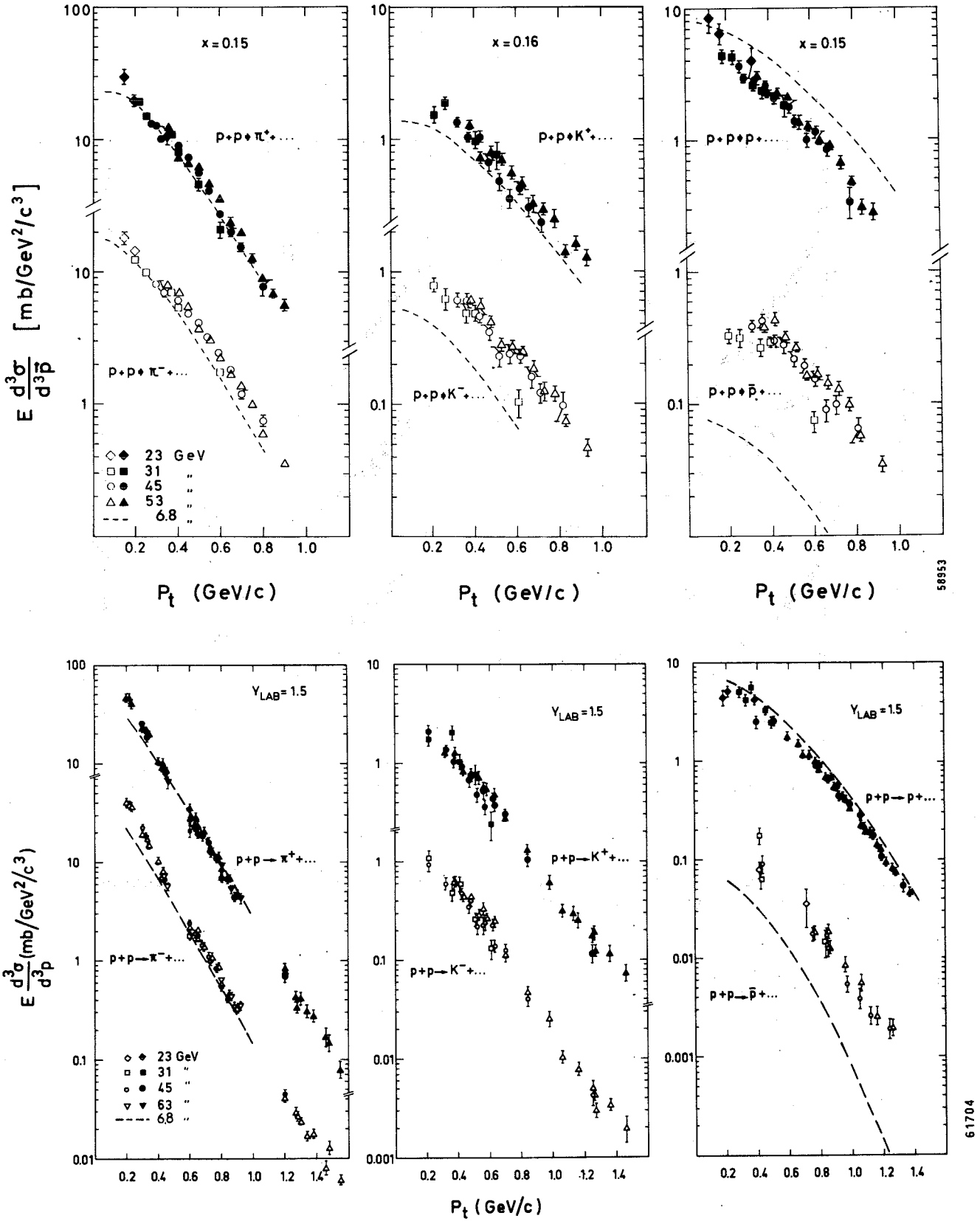

Fig. 3.3 The invariant cross-sections for π^+, π^-, K^+, K^-, p, and $\bar{p}$ production versus p_t at (a) x = 0.15 and (b) y_{lab} = 1.5 (Ref. 6)

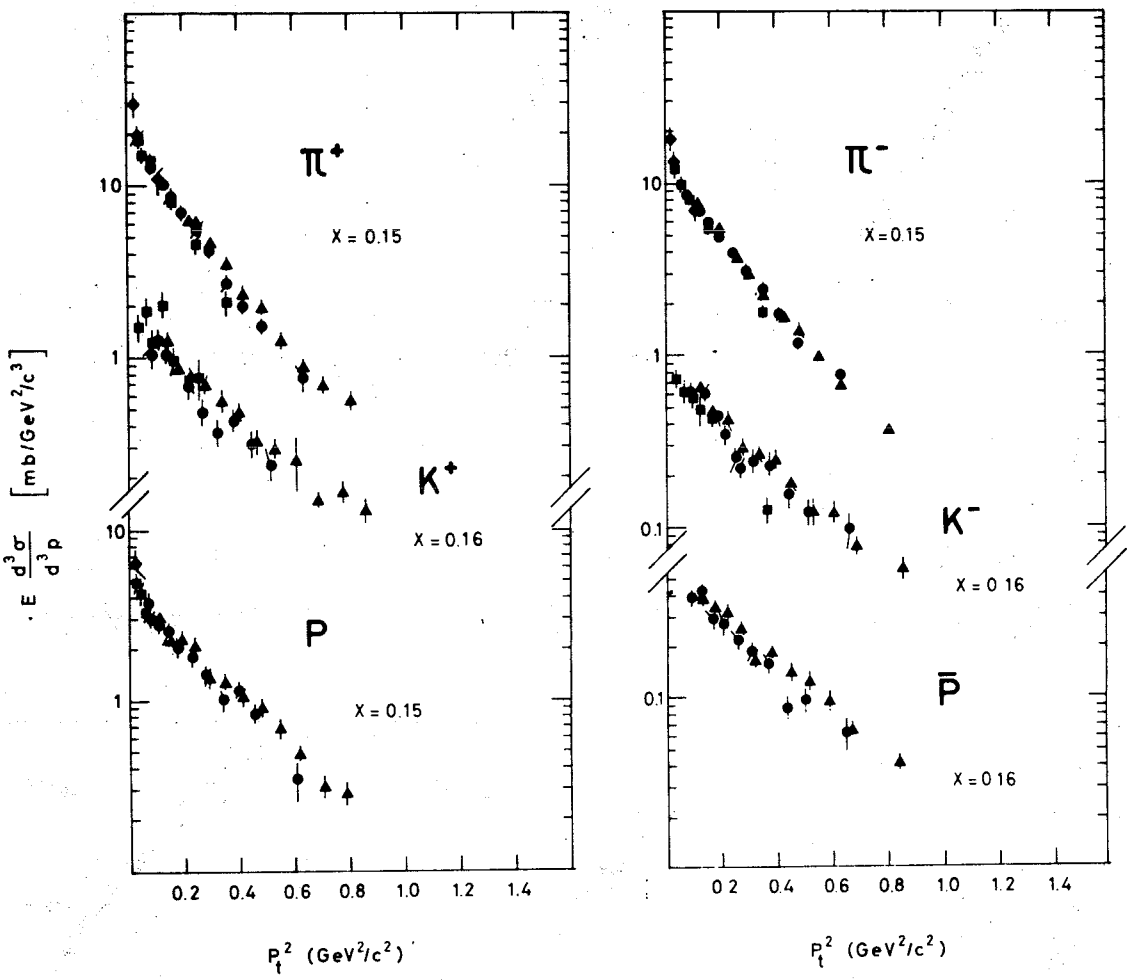

Fig. 4.1 The invariant cross-sections for π^+, π^-, K^+, K^-, p, and $\bar{p}$ production versus p_t^2 at x = 0.15 (Ref. 5)

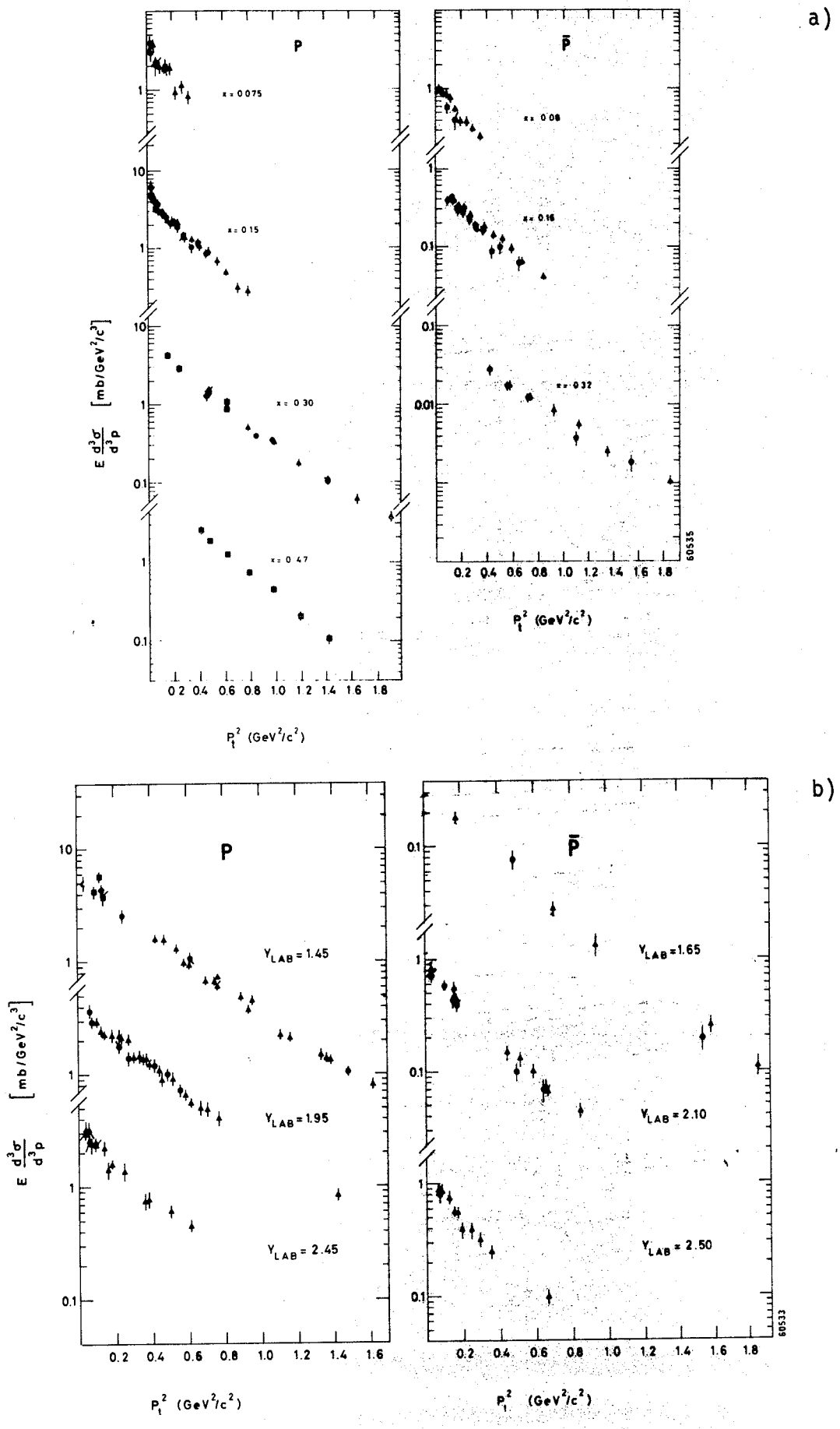

Fig. 4.2 The invariant cross-sections for p and $\bar{p}$ production (a) at fixed values of x and (b) at fixed values of y_{lab} versus p_t^2 (Ref. 5)

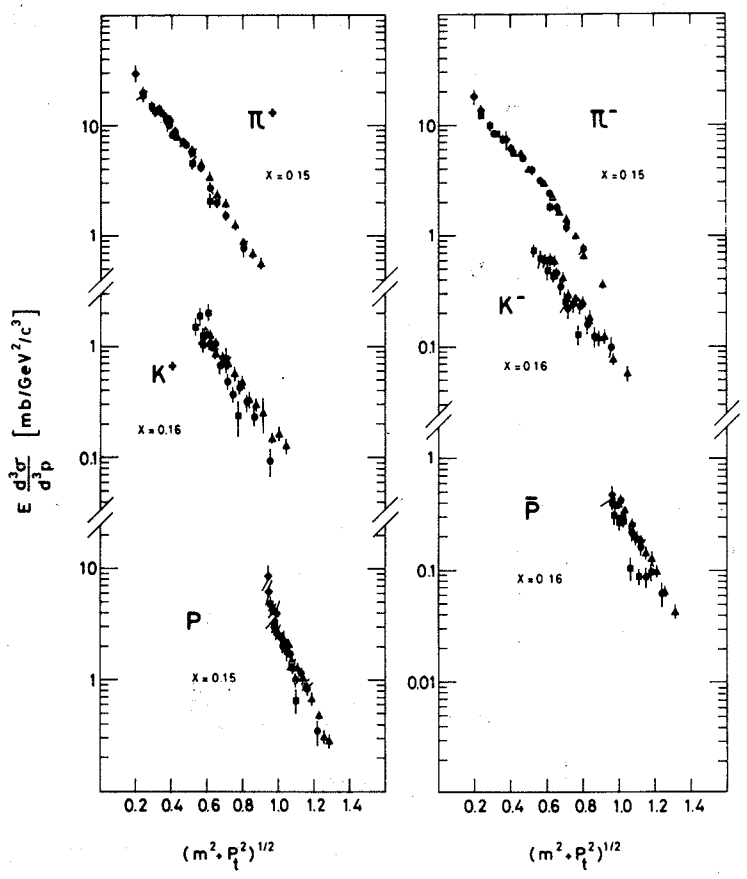

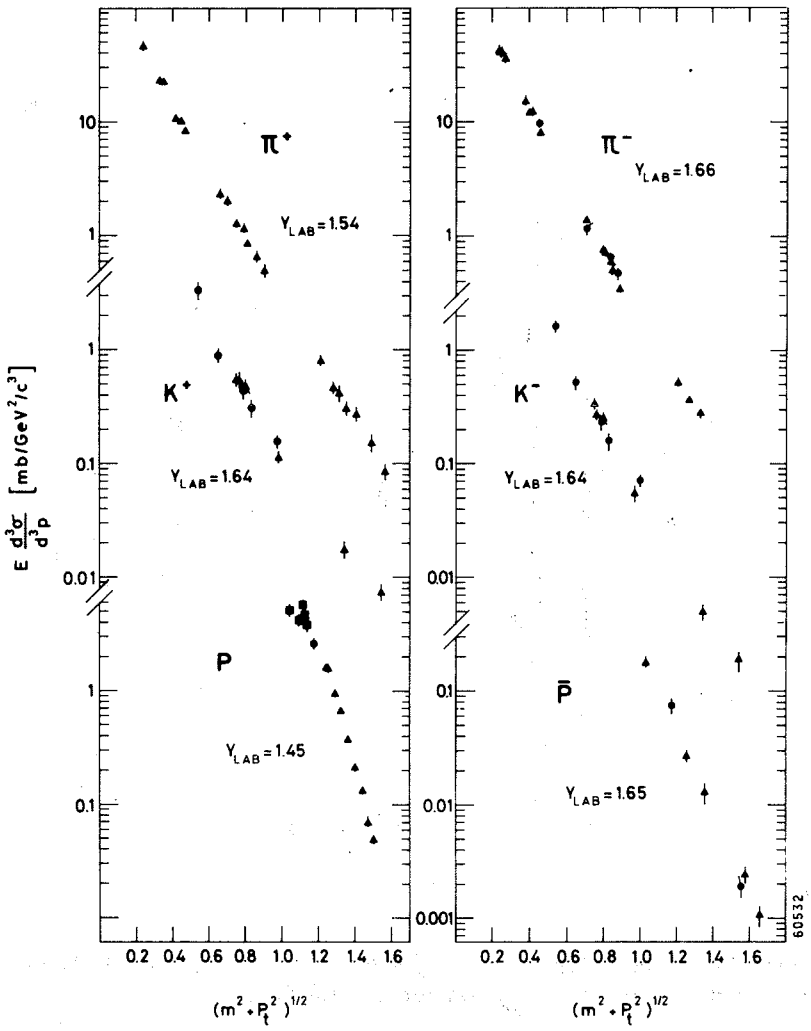

Fig. 5
The invariant cross-sections for π^+, π^-, K^+, K^-, p, and $\bar{p}$ production versus the longitudinal mass m_l, (a) at x = 0.15 (Ref. 5) and (b) at fixed values of y_{lab}

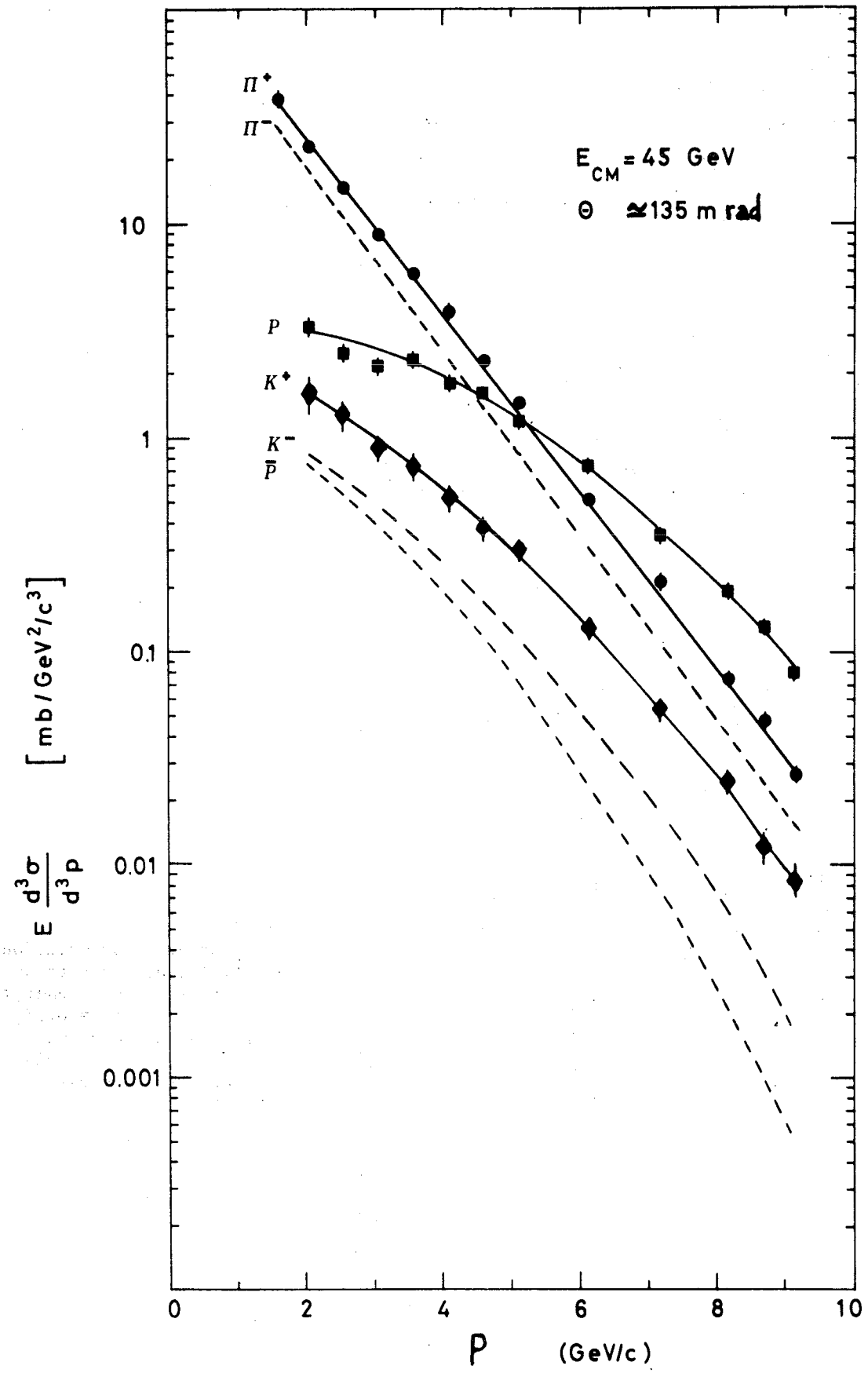

Fig. 6 The invariant cross-sections for π^+, π^-, K^+, K^-, p, and $\bar{p}$ production at the fixed production angle θ_{ISR} = 135 mrad, versus the particle momentum p in the ISR frame of reference. For clarity, the experimental points are not shown for negative particles. The lines are only meant to guide the eye (Ref. 5).

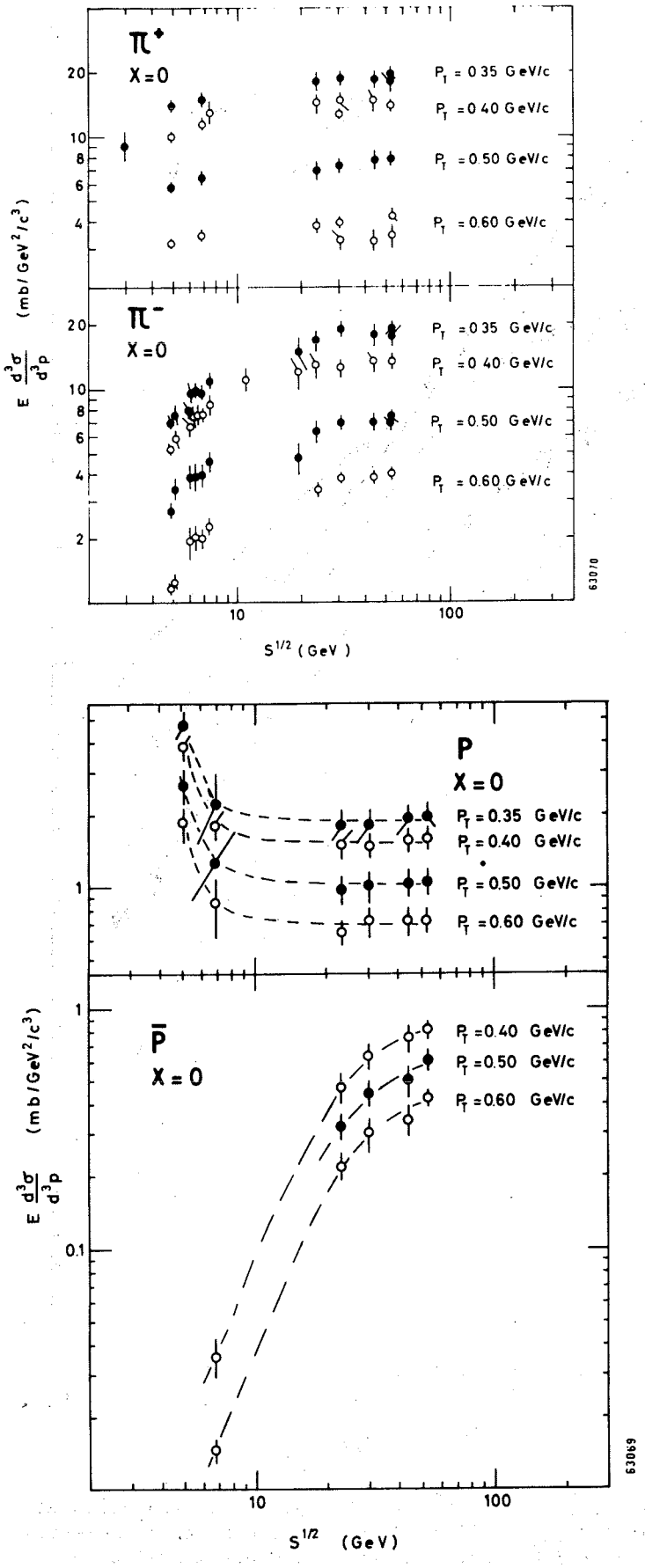

Fig. 7.1
The invariant cross-sections for π^+, π^-, p, and $\bar{p}$ production versus the c.m. energy $\sqrt{s}$ at x = 0 and p_t = 0.35, 0.40, 0.50, and 0.60 GeV/c. The dashed lines are only meant to guide the eye (Ref. 7).

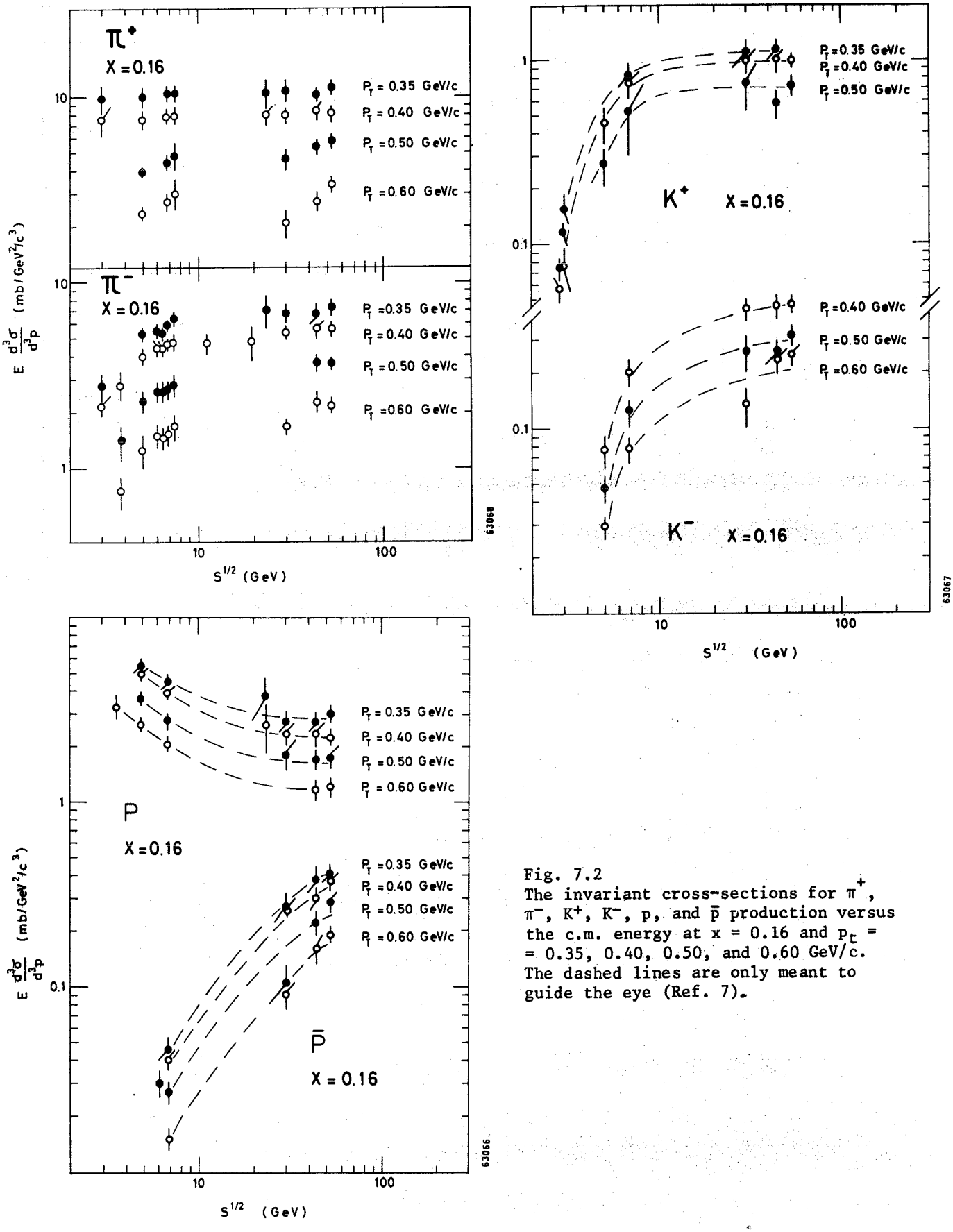

Fig. 7.2
The invariant cross-sections for π^+, π^-, K^+, K^-, p, and $\bar{p}$ production versus the c.m. energy at x = 0.16 and p_t = = 0.35, 0.40, 0.50, and 0.60 GeV/c. The dashed lines are only meant to guide the eye (Ref. 7).

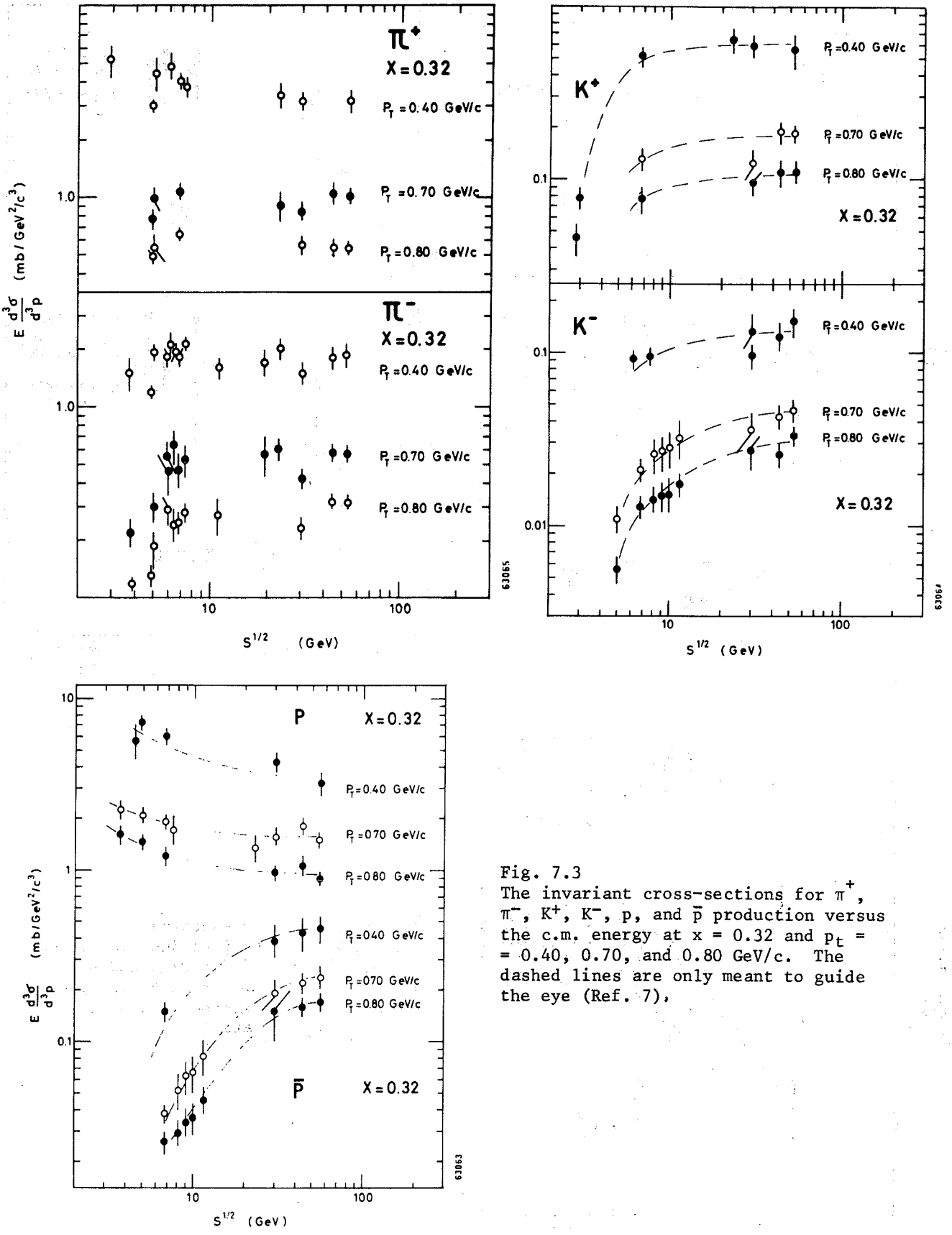

Fig. 7.3
The invariant cross-sections for π^+, π^-, K^+, K^-, p, and $\bar{p}$ production versus the c.m. energy at x = 0.32 and p_t = = 0.40, 0.70, and 0.80 GeV/c. The dashed lines are only meant to guide the eye (Ref. 7).

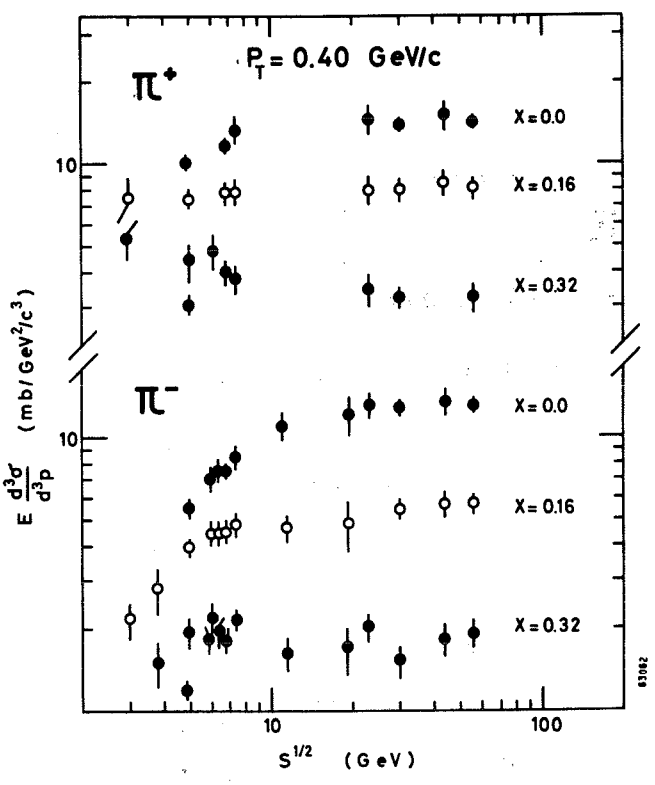

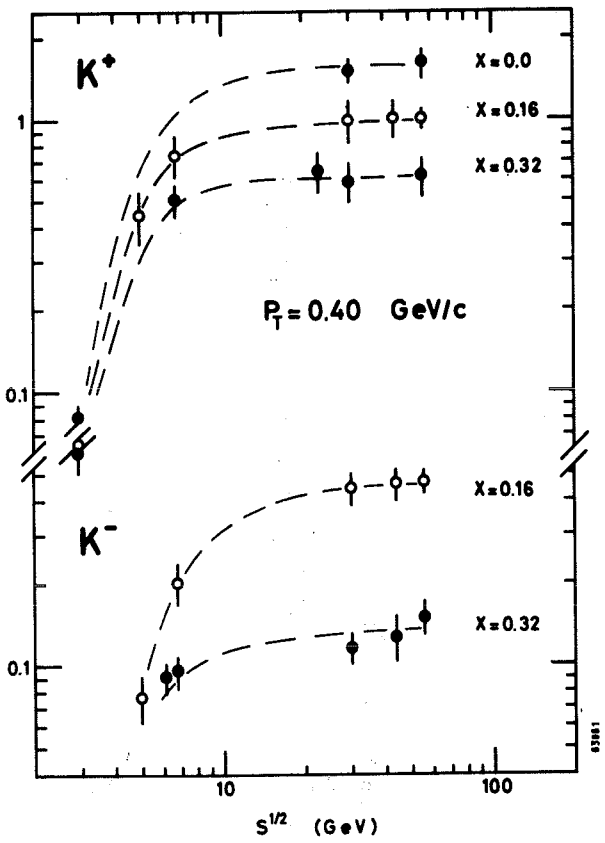

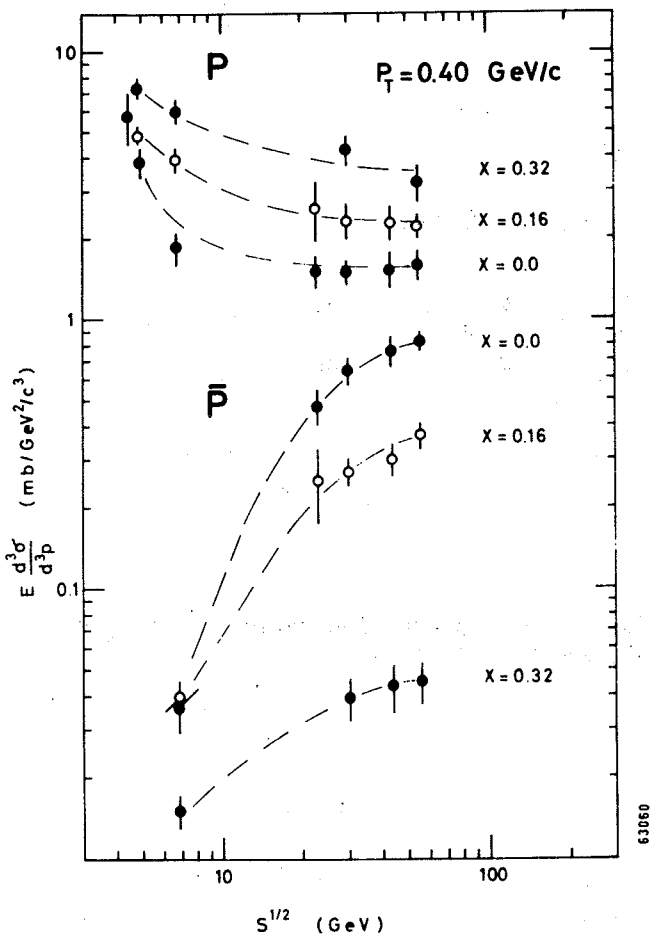

Fig. 7.4
The invariant cross-sections for π^+, π^-, K^+, K^-, p, and $\bar{p}$ production versus the c.m. energy at p_t = 0.40 GeV/c and x = 0.0, 0.16, and 0.32. The dashed lines are only meant to guide the eye (Ref. 7).

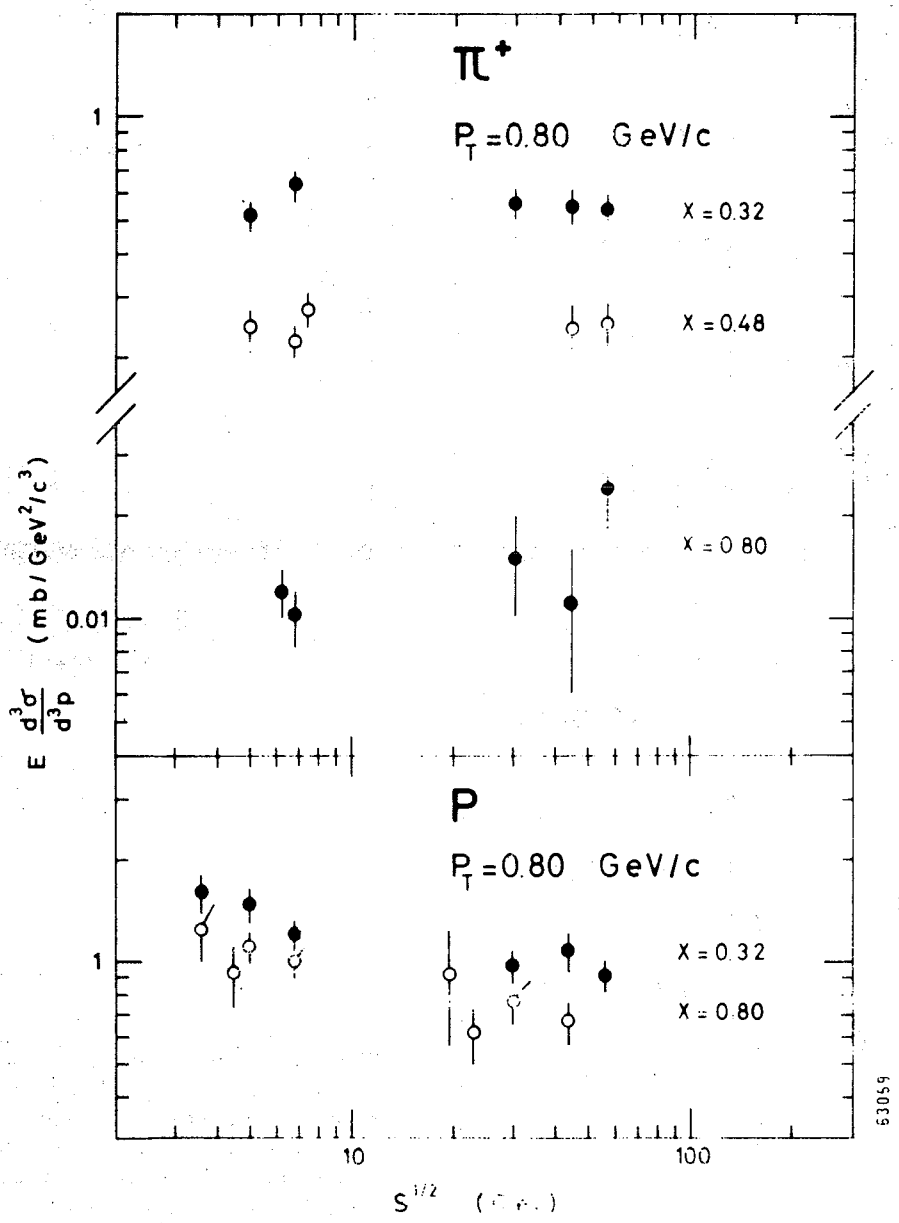

Fig. 7.5 The invariant cross-sections for π^+ and p production versus $\sqrt{s}$ at p_t = = 0.80 GeV/c and x = 0.32, 0.48, and 0.80 (Ref. 7)

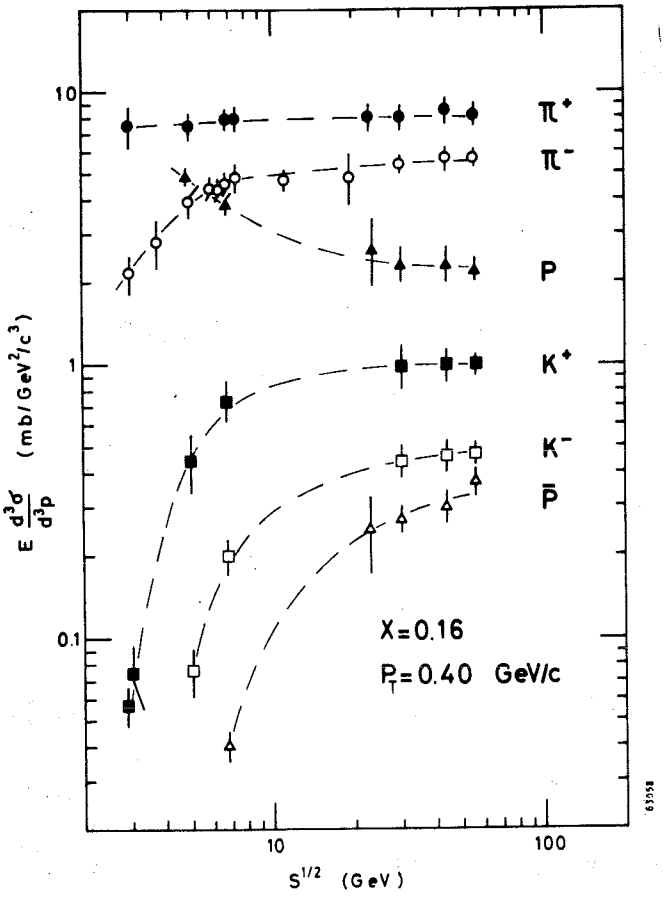

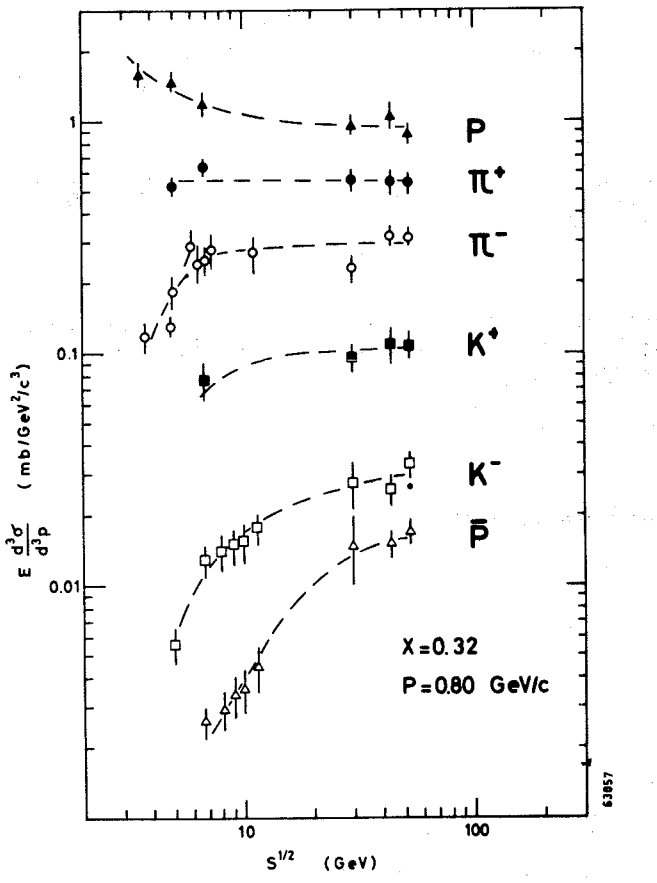

Fig. 7.6
The invariant cross-sections for π^+, π^-, K^+, K^-, p, and $\bar{p}$ production versus $\sqrt{s}$ at (a) x = 0.16, p_t = 0.40 GeV/c and (b) x = 0.32, p_t = 0.80 GeV/c. The dashed lines are only meant to guide the eye (Ref. 7).

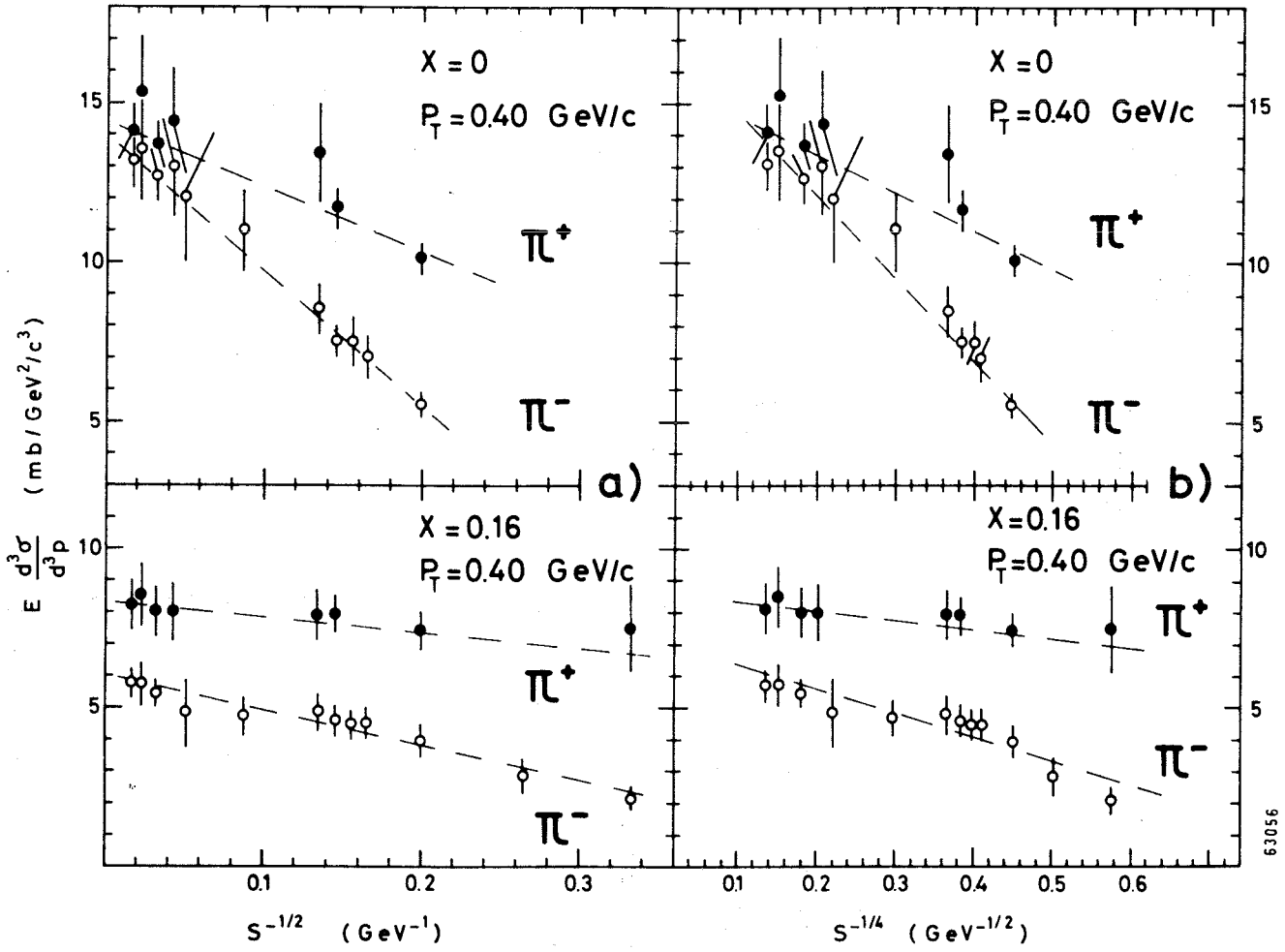

Fig. 7.7 The invariant cross-sections for π^+ and π^- production at p_t = 0.40 GeV/c and x = 0.0 and 0.16 versus (a) $s^{-\frac{1}{2}}$ and (b) $s^{-\frac{1}{4}}$. The dashed lines represent the results of fits (Ref. 7).

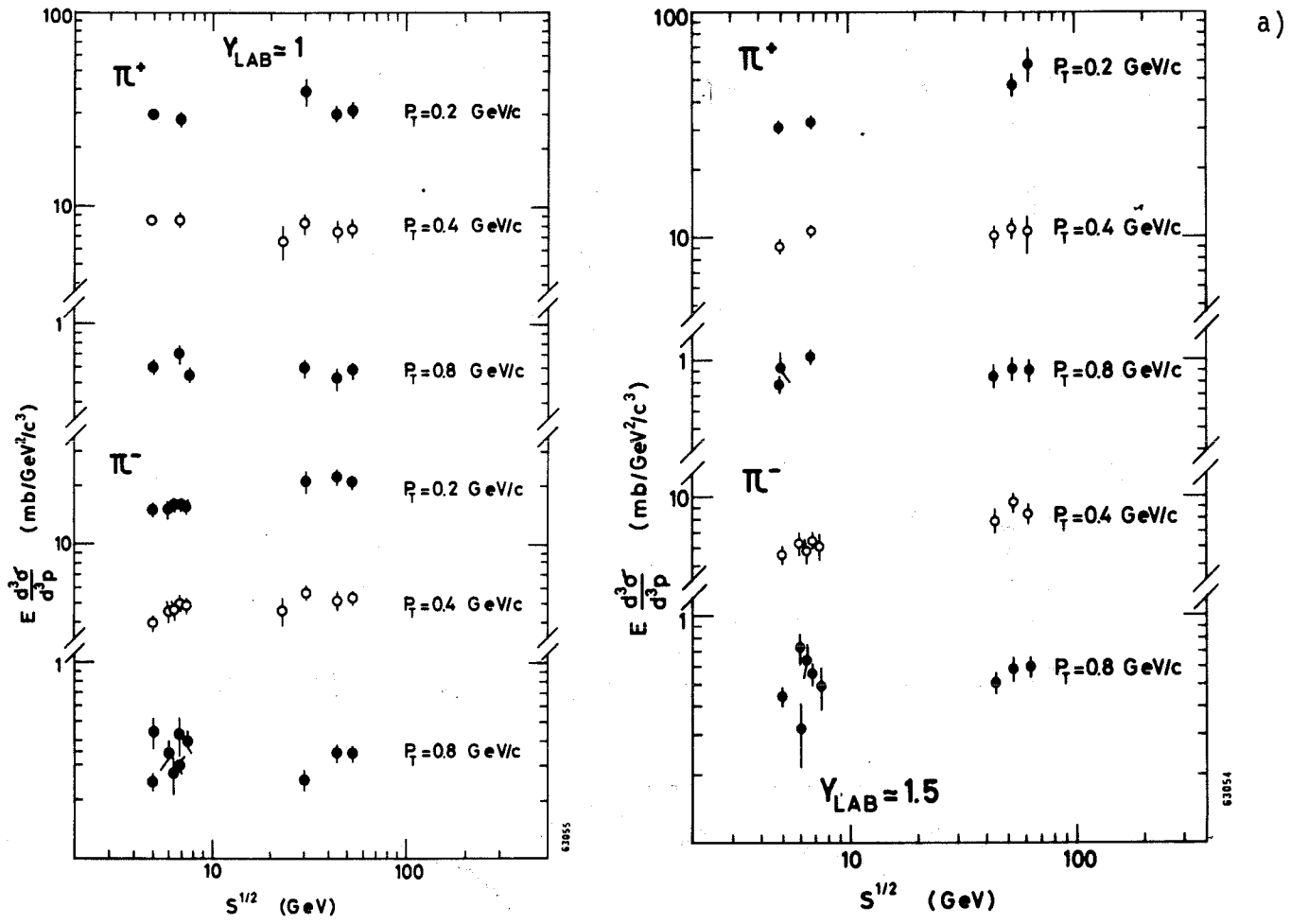

Fig. 7.8
The invariant cross-sections (a) for π^+ and π^- production versus $\sqrt{s}$ at $y_{lab} \simeq 1$ and 1.5 and p_t = 0.2, 0.4, and 0.8 GeV/c (Ref. 7); (b) for K^+ and p at y_{lab} = 1 and p_t = 0.4 and 0.8 GeV/c.

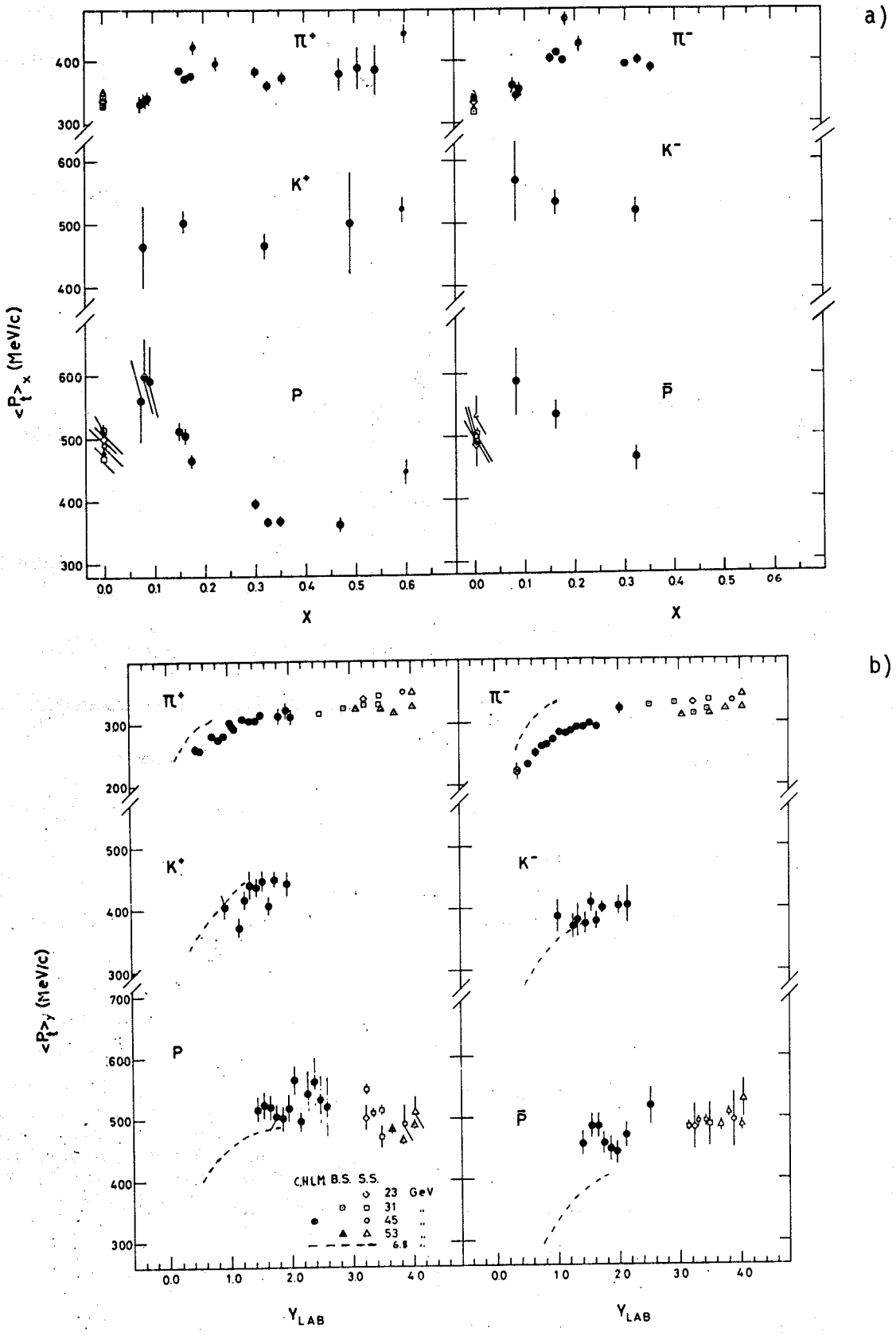

Fig. 8 Compilation of the average values of the transverse momentum for π^+, π^-, K^+, K^-, p, and $\bar{p}$, computed (a) at fixed values of x and $\langle p_t \rangle_x$, and (b) at fixed values of y_{lab} and $\langle p_t \rangle_y$ (Ref. 5)

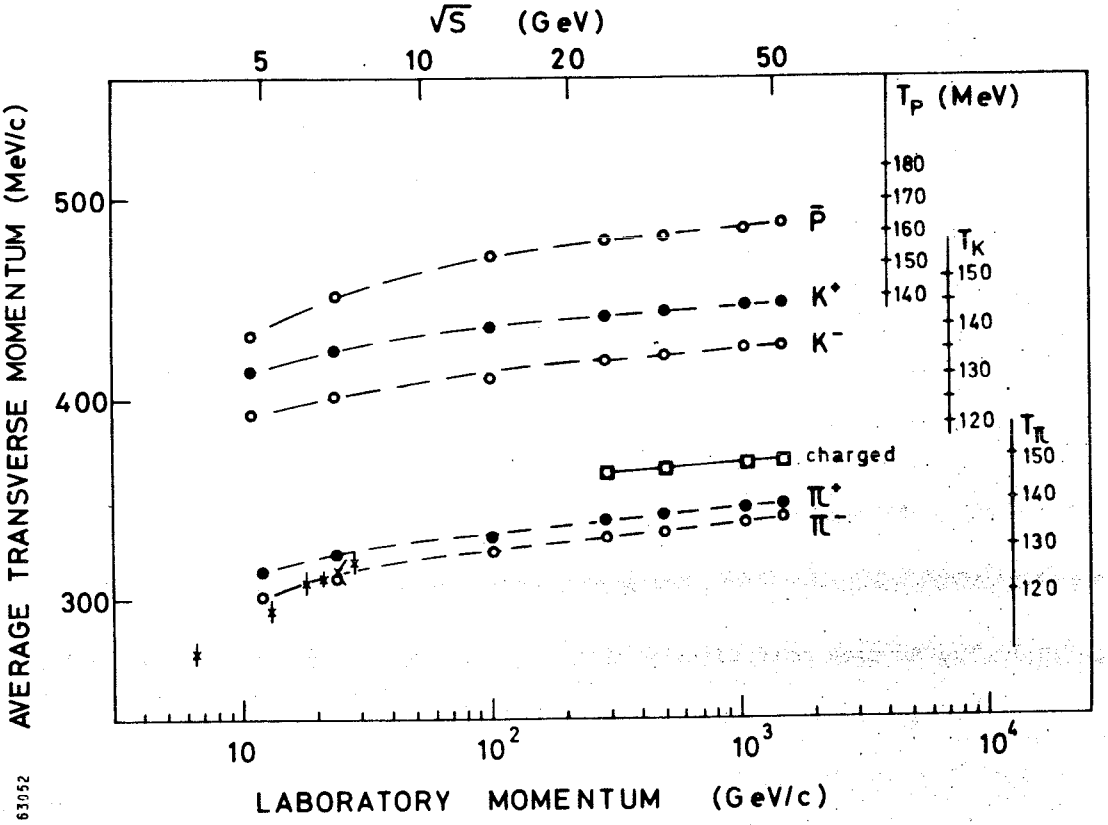

Fig. 9 Average transverse momentum for the production of pions, kaons, antiprotons and all charged particles versus laboratory momentum. On the right are shown "temperature" scales for different particles (Ref. 7).

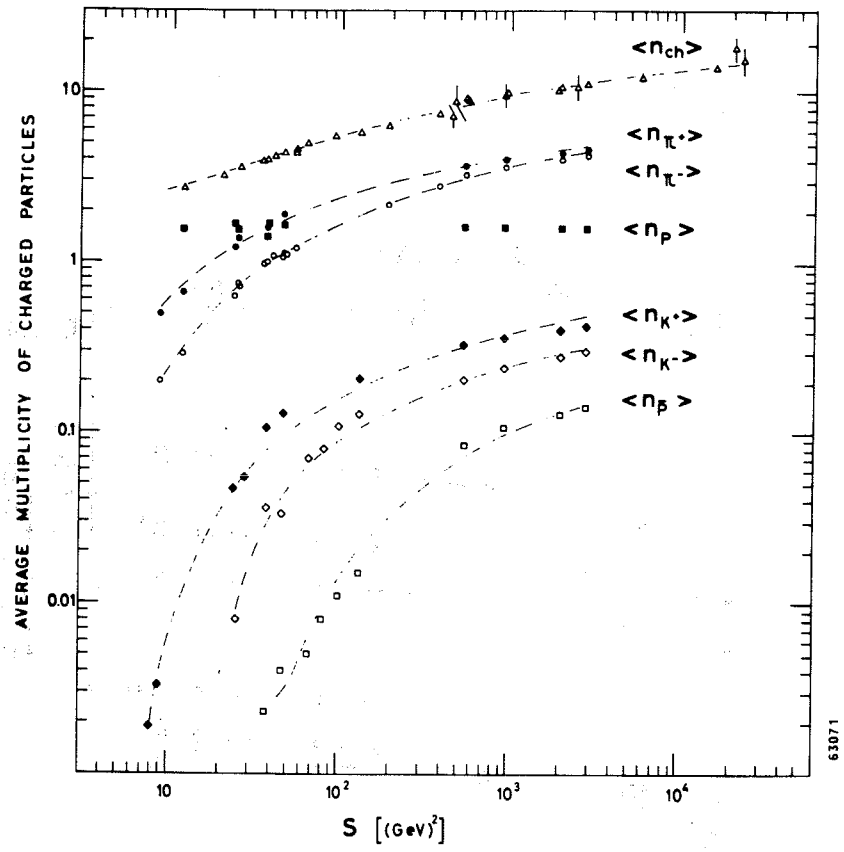

Fig. 10.1 The average multiplicity of π^+, π^-, K^+, K^-, p, $\bar{p}$, and all charged particles, plotted as a function of s, the square of c.m. energy. Dashed lines represent the results of the fits (Ref. 7).

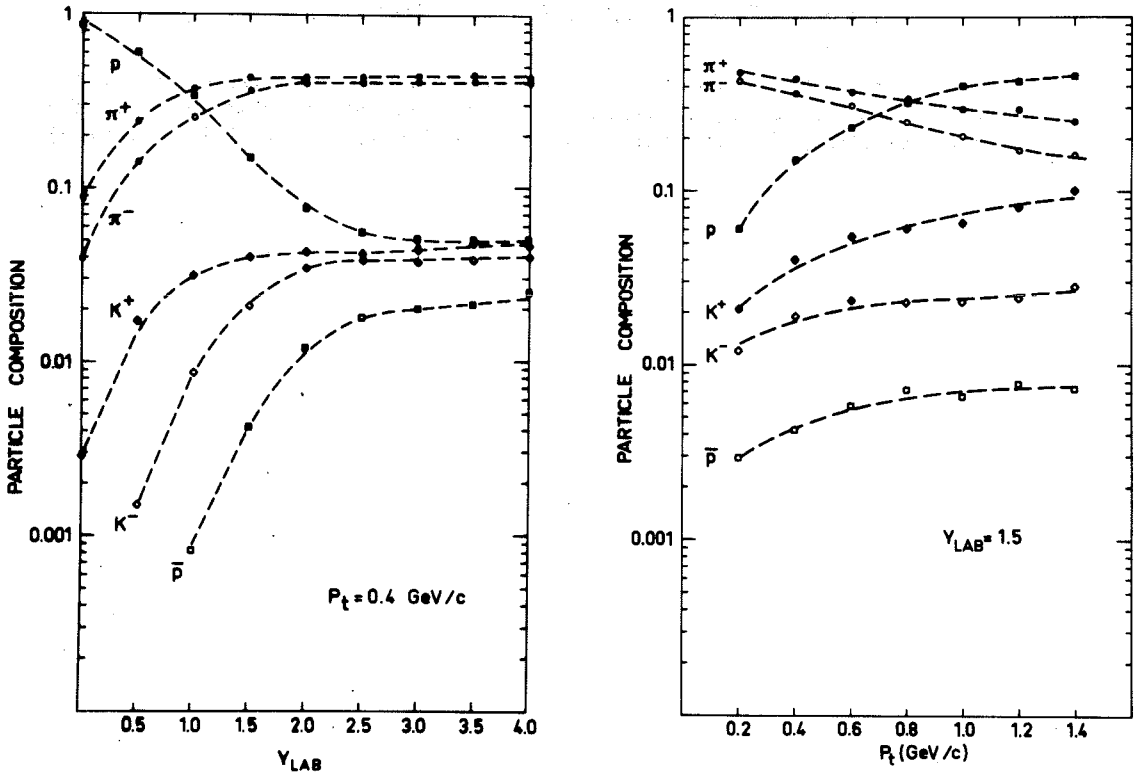

Fig. 10.2a Particle composition as a function of y_{lab} and p_t. The dashed lines are only meant to guide the eye (Ref. 6).

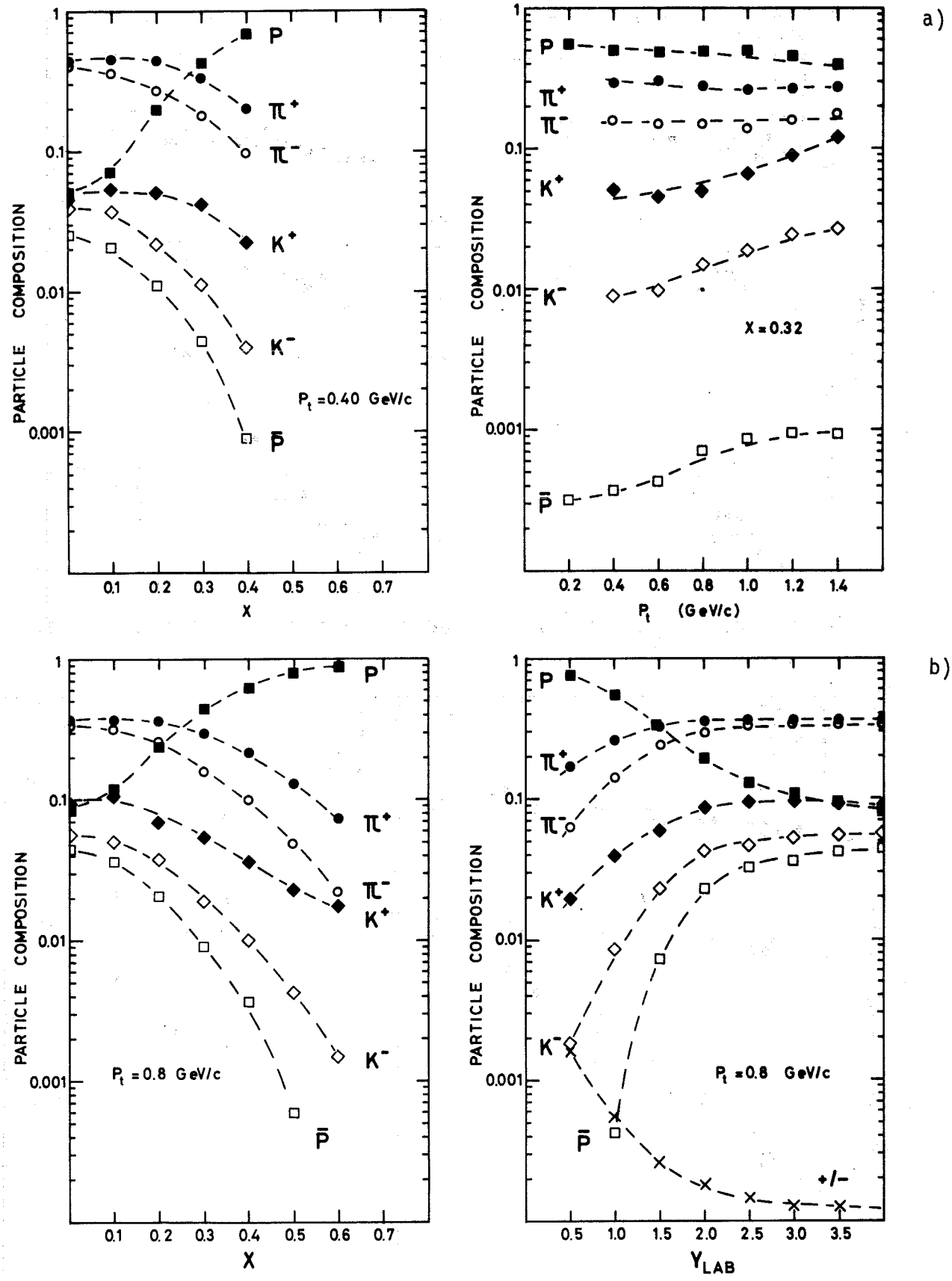

Fig. 10.2b Particle composition versus x for p_t = 0.4 and versus p_t for x = 0.32; versus x and versus y_{lab} for p_t = 0.8.

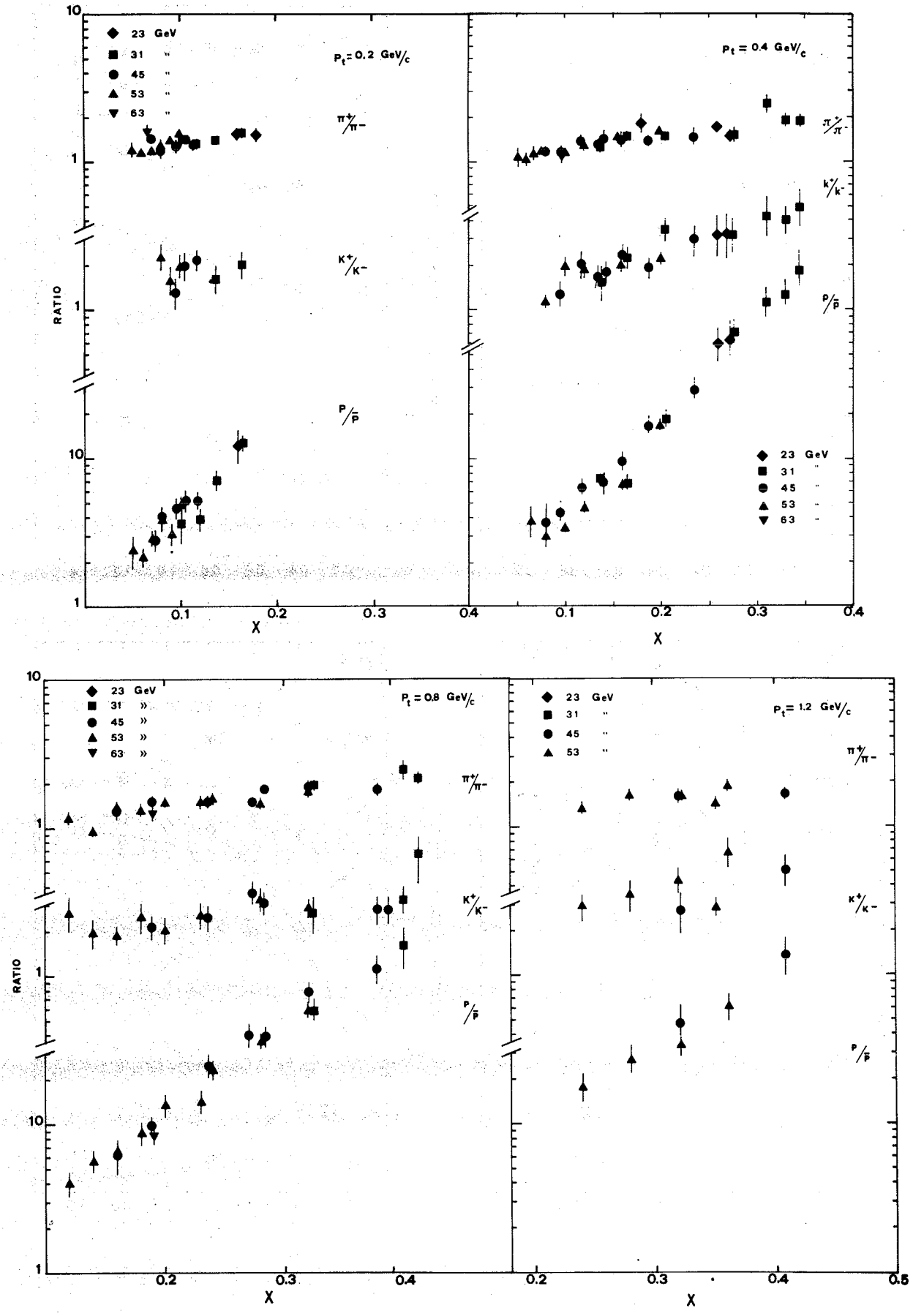

Fig. 11.1 Particle-to-antiparticle ratios versus x at p_t = 0.2, 0.4, 0.8, and 1.2 GeV/c. (See Table 1 for numerical values.)

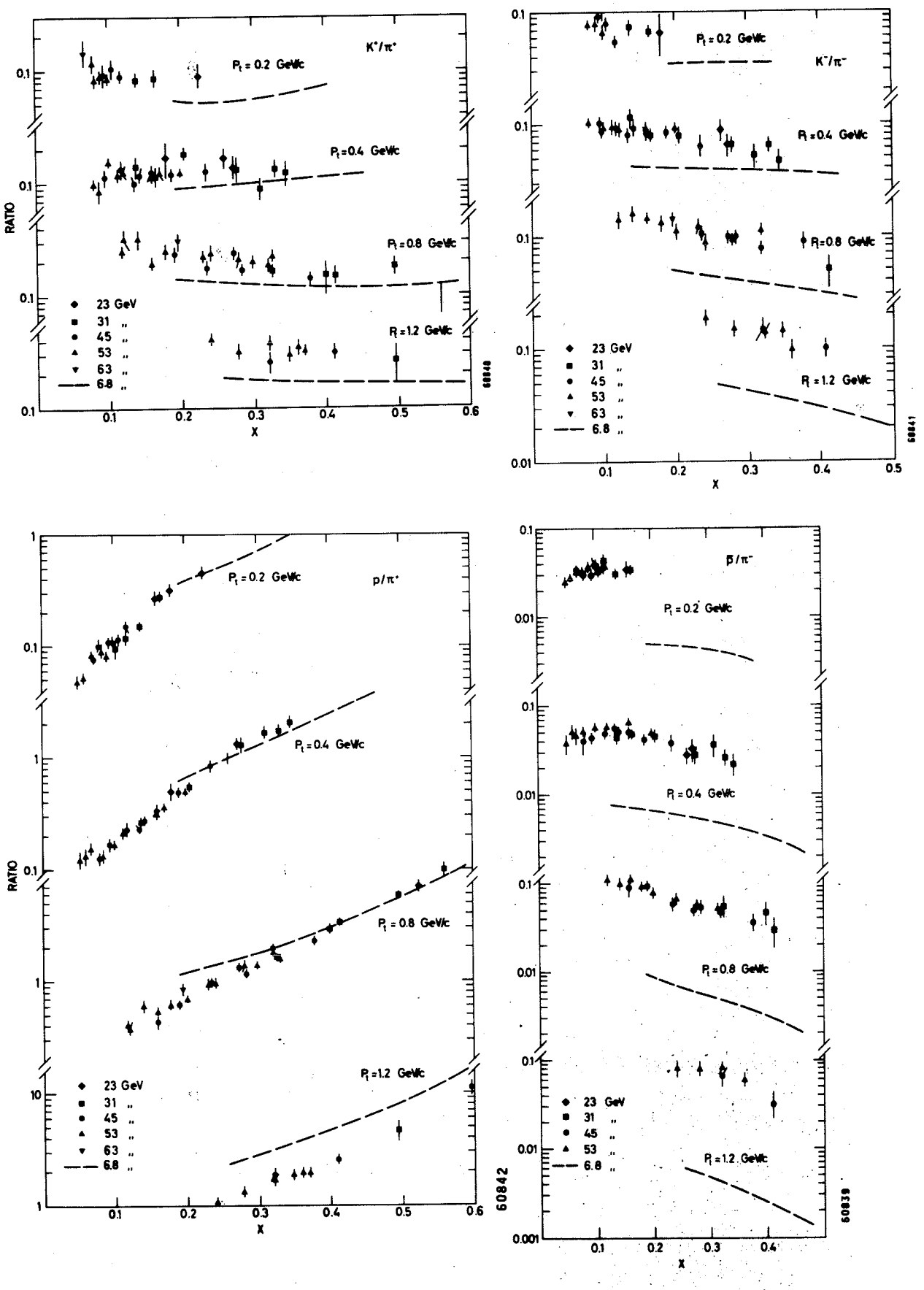

Fig. 11.2 Particle-to-pion of the same charge ratios versus x at p_t = 0.2, 0.4, 0.8, and 1.2 GeV/c (Table 2, Ref. 6)

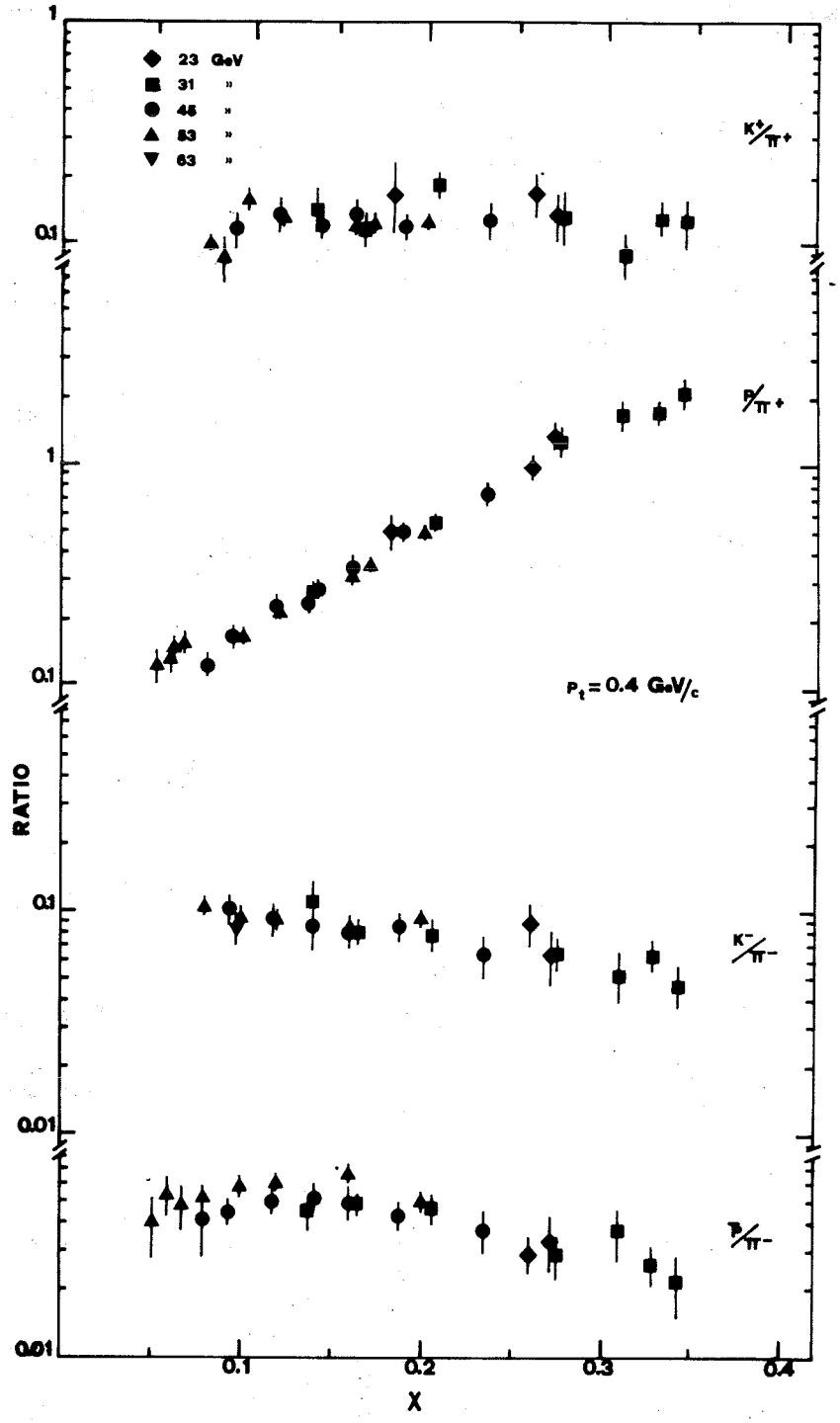

Fig. 11.3 Particle-to-pion of the same charge ratios versus x at p_t = 0.4 GeV/c (Table 2)

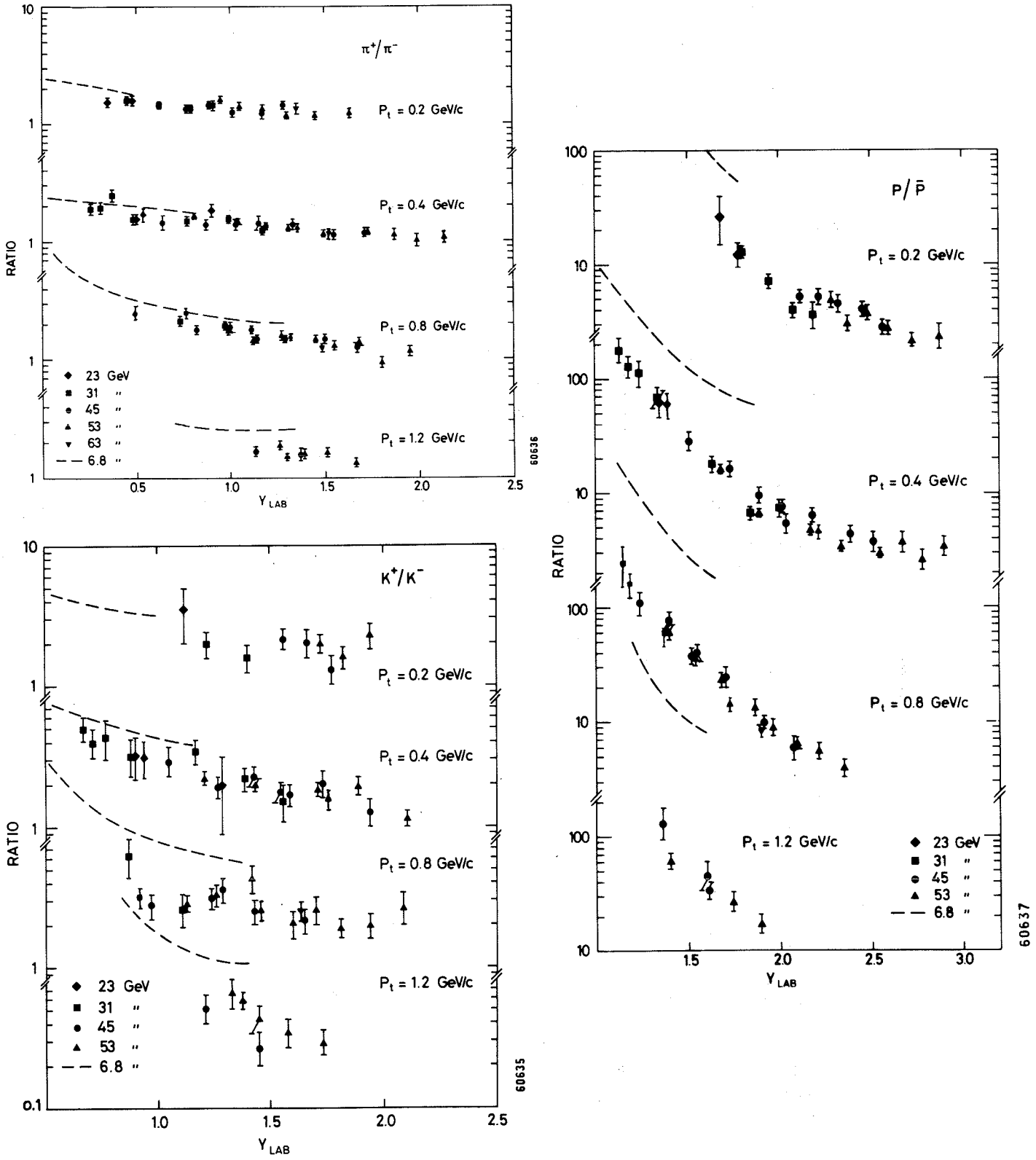

Fig. 12.1 Particle-to-antiparticle ratios versus y_{lab} at p_t = 0.2, 0.4, 0.8, and 1.2 GeV/c (Table 3, Ref. 6)

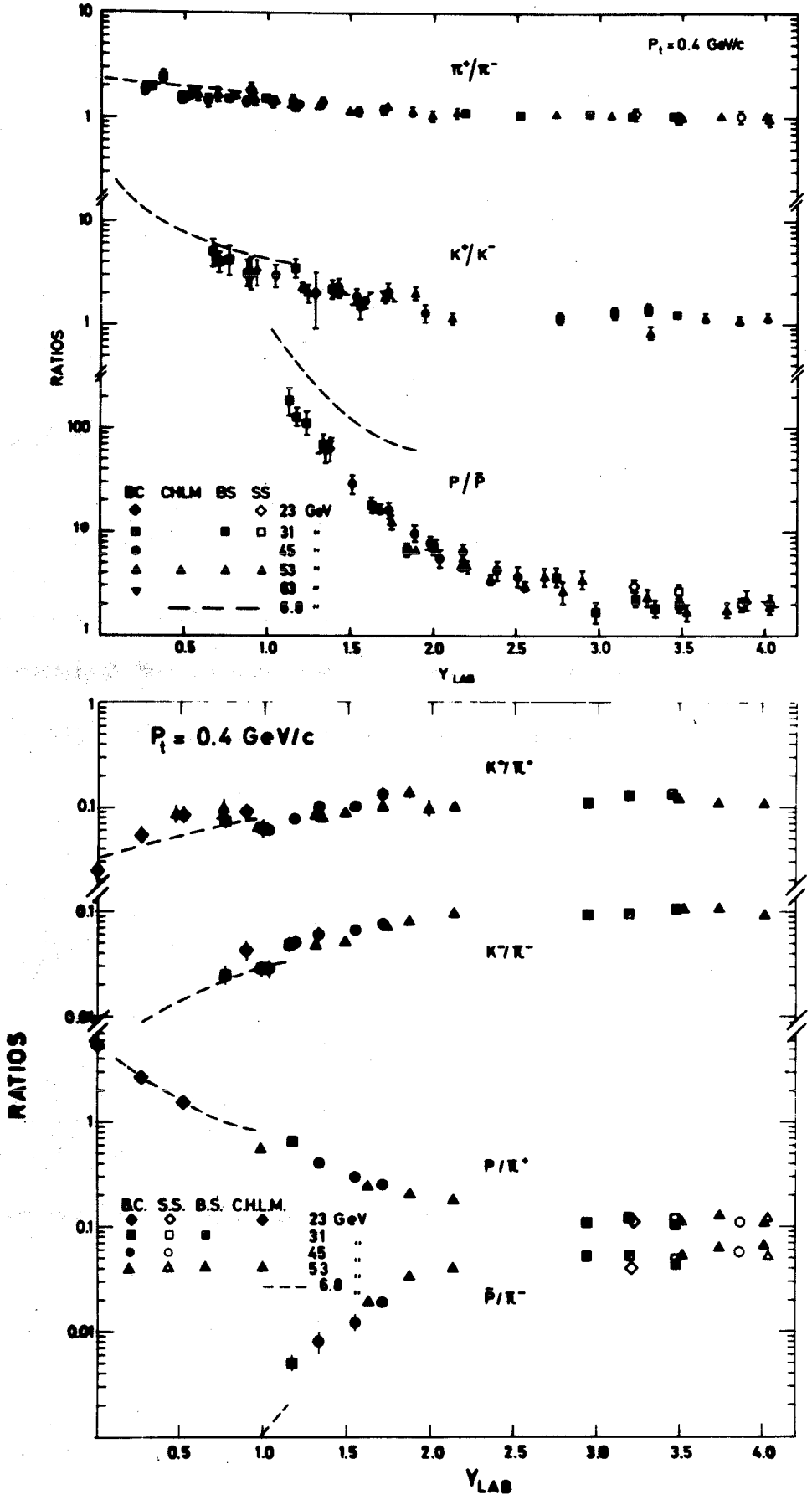

Fig. 12.2 Particle-to-antiparticle and particle-to-pion of the same charge ratios versus y_{lab} at p_t = 0.4 GeV/c (Tables 3 and 4, Ref. 6)

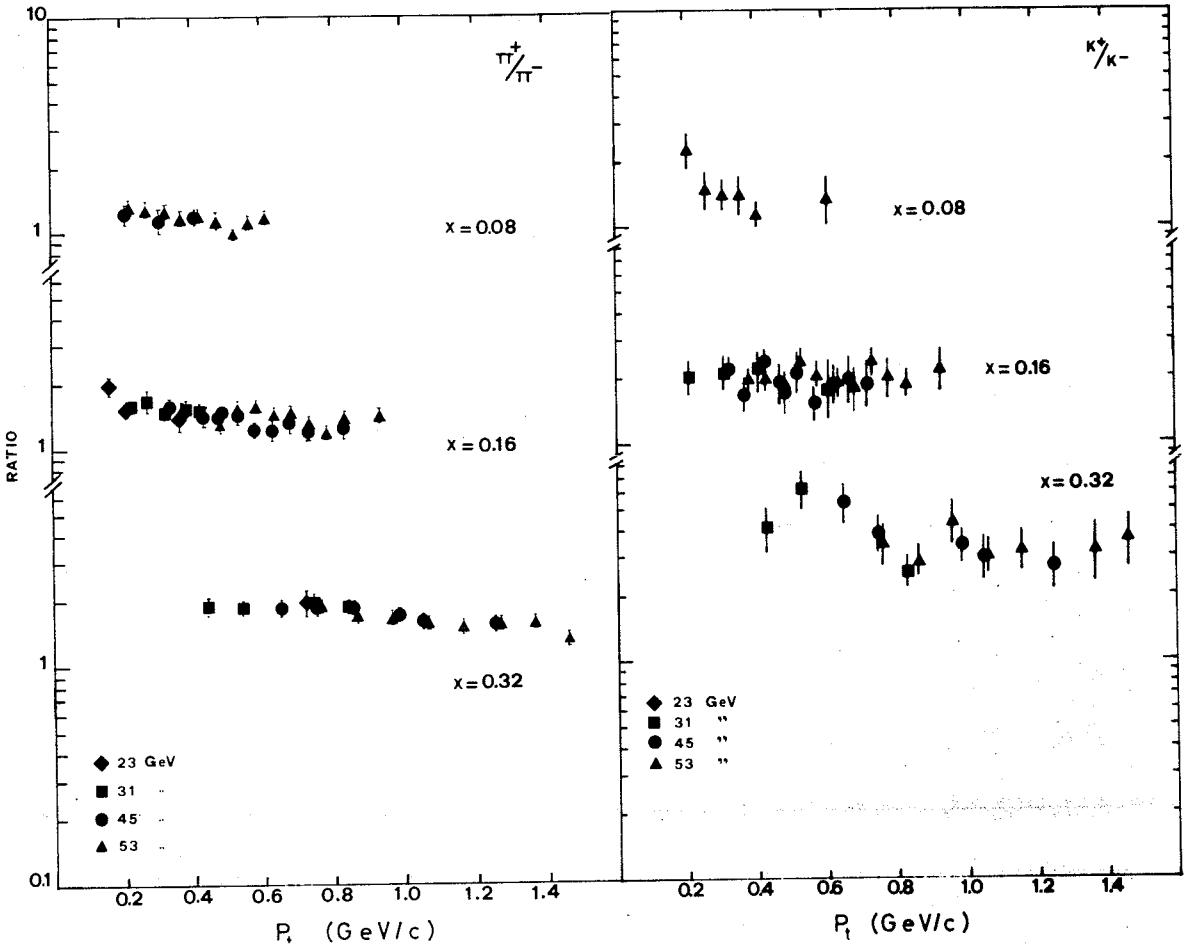

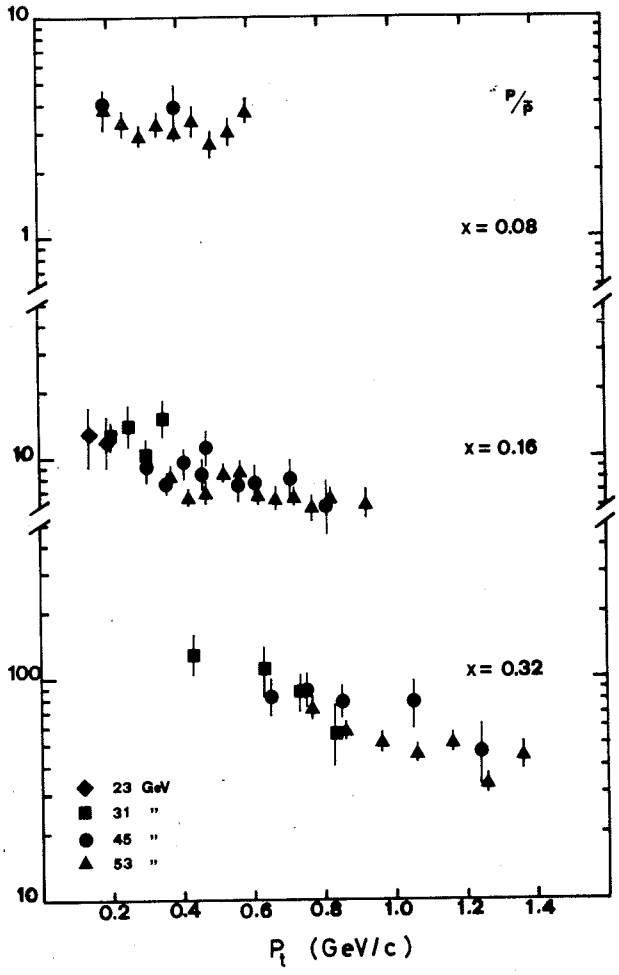

Fig. 13.1
Particle-to-antiparticle ratios versus p_t at x = 0.08, 0.16, and 0.32 (Table 5)

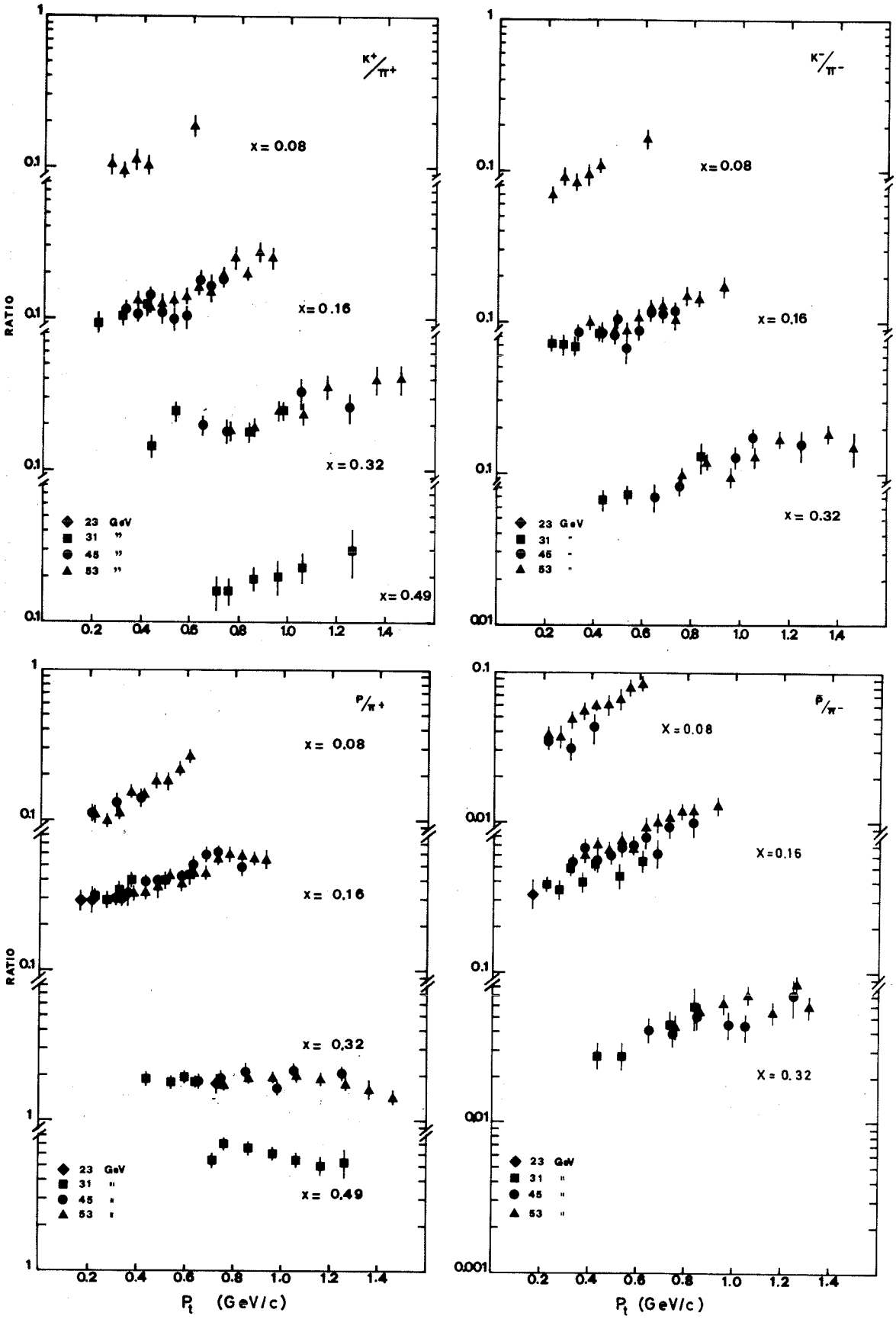

Fig. 13.2 Particle-to-pion of the same charge ratios versus p_t at x = 0.08, 0.16, and 0.32 (Table 6)

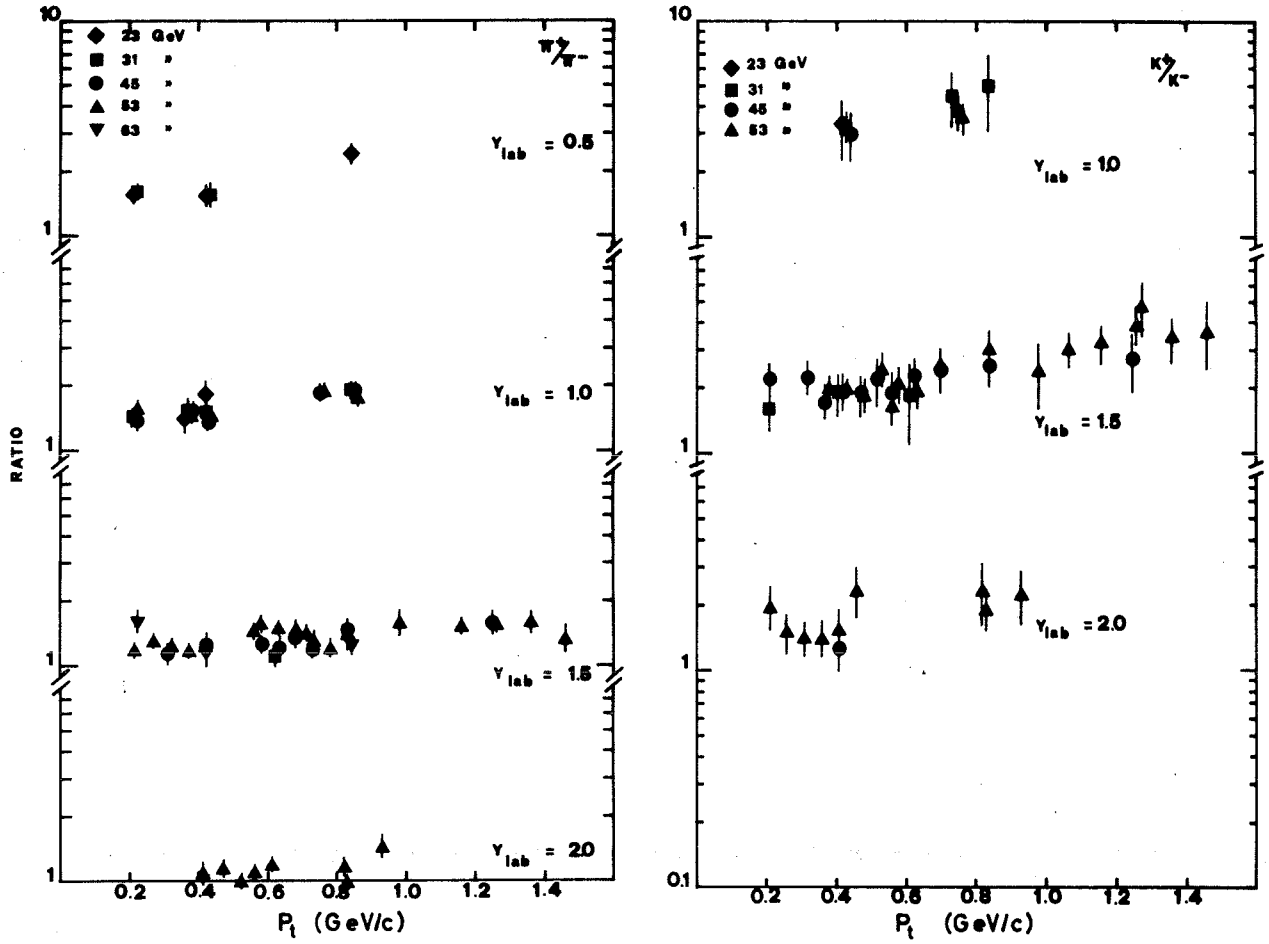

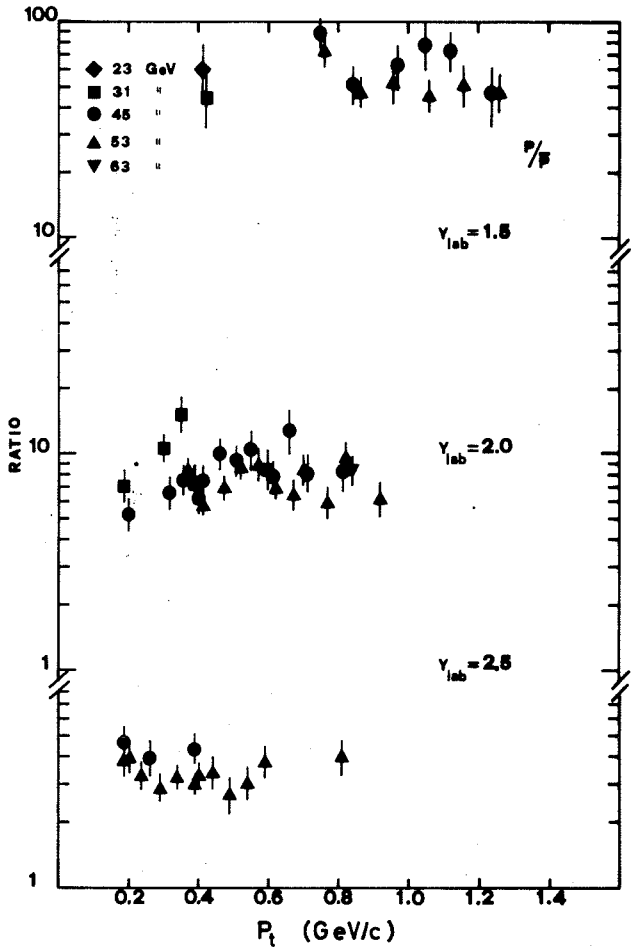

Fig. 13.3
Particle-to-antiparticle ratios versus p_t at y_{lab} = 0.5, 1.0, 1.5, 2.0, and 2.5 (Table 7)

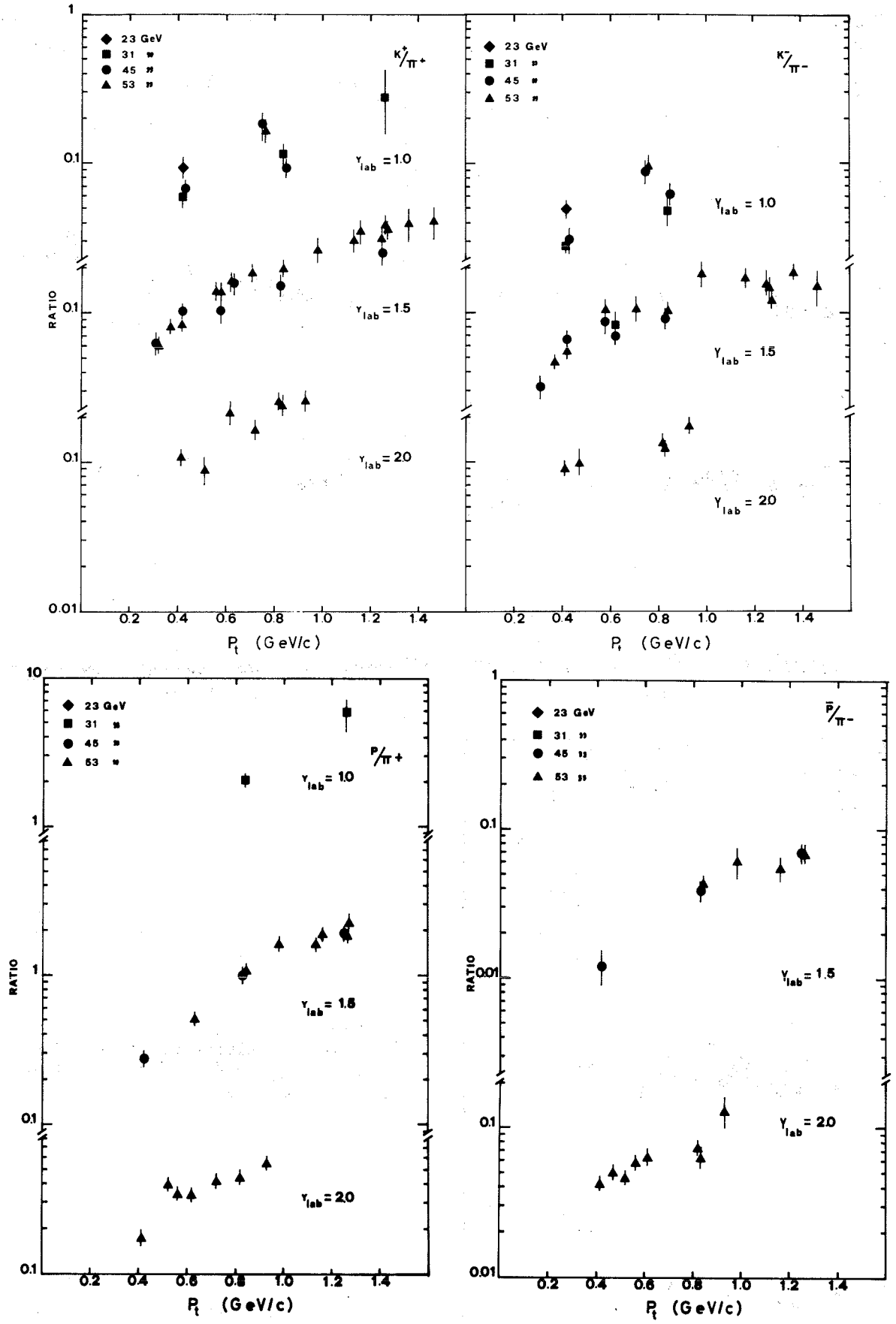

Fig. 13.4 Particle-to-pion of the same charge ratios versus p_t at y_{lab} = 1.0, 1.5, and 2.0 (Table 8)

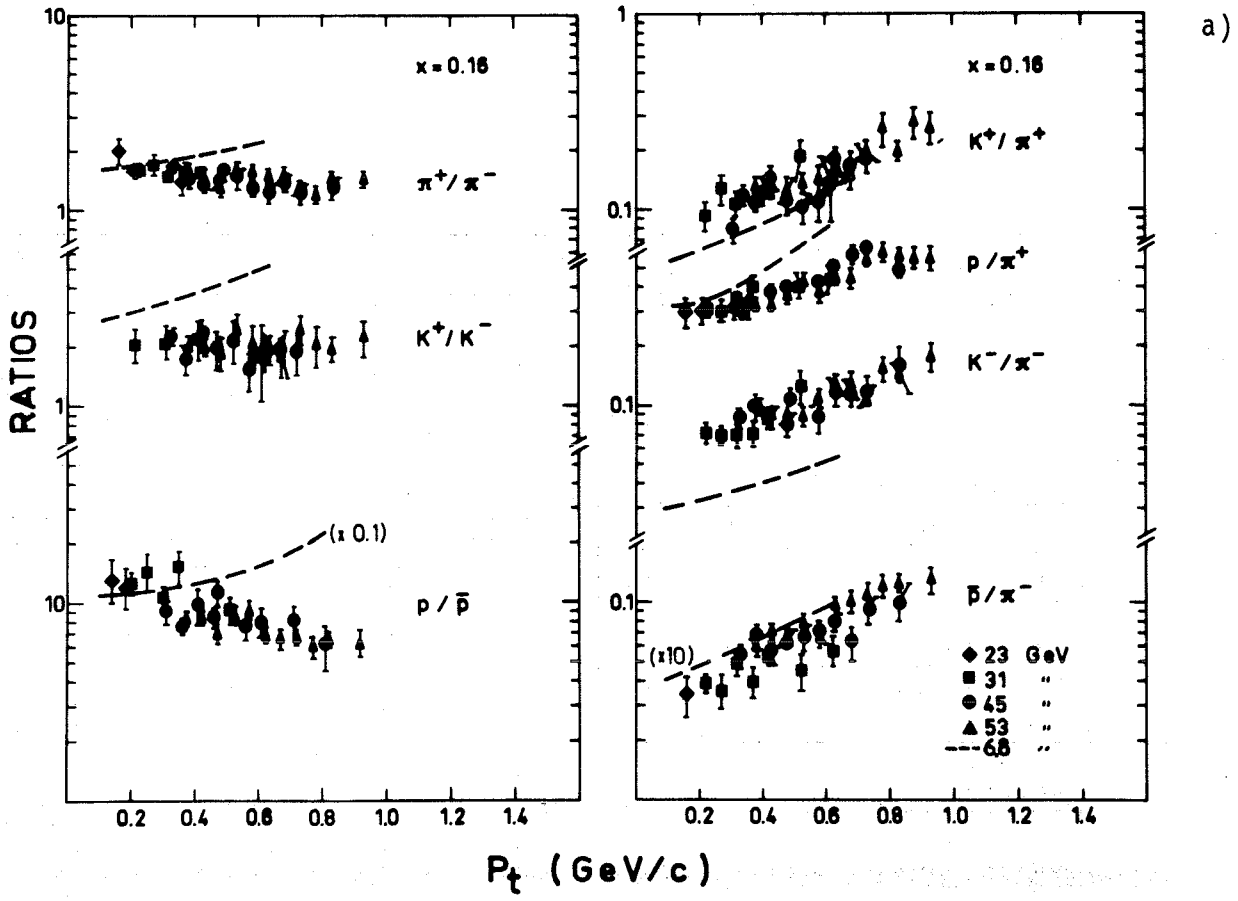

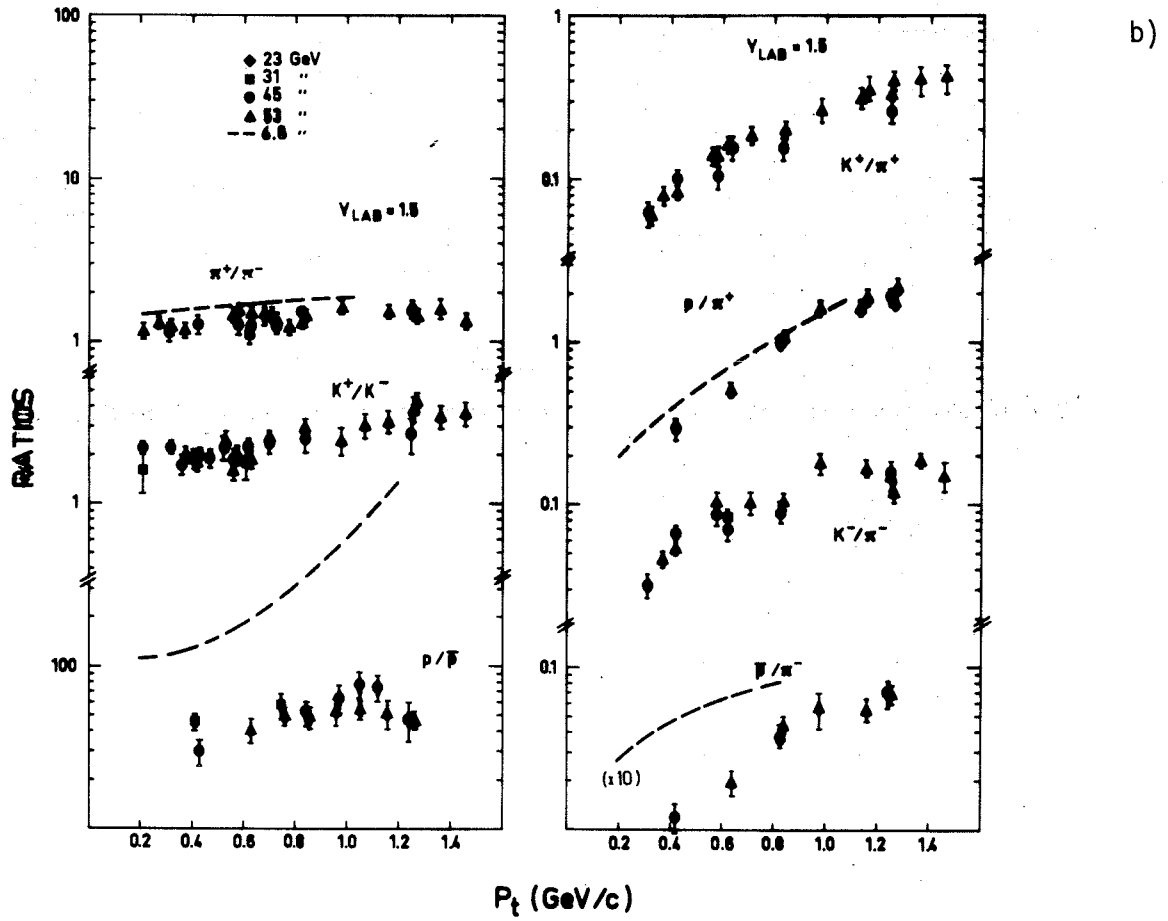

Fig. 13.5 Particle-to-antiparticle and particle-to-pion of the same charge ratios versus p_t at (a) x = 0.16 and (b) y_{lab} = 1.5 (Tables 5-8, Ref. 6)

$\sqrt{s}$ (GeV)	p_T (GeV/c)	y_{lab}	$R(\pi^+/\pi^-)$	y_{lab}	$R(K^+/K^-)$	y_{lab}	$R(p/\bar{p})$
23	0.20	0.49	1.58 ± 0.15	1.10	3.60 ± 1.6	1.8	12.4 ± 3.0
		0.35	1.54 ± 0.15				
31	0.20	0.91	1.45 ± 0.13	1.4	1.62 ± 0.34	2.2	3.68 ± 1.0
		0.79	1.34 ± 0.097	1.2	2.04 ± 0.39	2.1	3.88 ± 0.60
		0.62	1.42 ± 0.061			1.9	7.15 ± 1.1
		0.45	1.60 ± 0.11			1.8	12.9 ± 1.7
45	0.20	1.3	1.44 ± 0.088	1.8	1.32 ± 0.31	2.6	2.86 ± 0.45
		1.2	1.22 ± 0.14	1.7	2.03 ± 0.45	2.5	4.10 ± 0.60
		1.0	1.28 ± 0.085	1.6	2.12 ± 0.36	2.3	4.62 ± 0.77
		0.89	1.46 ± 0.081			2.2	5.29 ± 0.83
		0.78	1.31 ± 0.074			2.1	5.27 ± 0.64
53	0.20	1.6	1.22 ± 0.12	1.9	2.32 ± 0.47	2.9	2.39 ± 0.60
		1.5	1.17 ± 0.074	1.8	1.60 ± 0.32	2.7	2.18 ± 0.30
		1.3	1.19 ± 0.077	1.7	2.01 ± 0.34	2.6	2.81 ± 0.40
		1.2	1.32 ± 0.087			2.5	3.80 ± 0.57
		1.1	1.41 ± 0.091			2.4	3.11 ± 0.52
		0.95	1.59 ± 0.096			2.3	4.96 ± 0.67
63	0.20	1.3	1.64 ± 0.18				
23	0.40	0.90	1.84 ± 0.27	0.93	3.30 ± 1.0	1.4	60.0 ± 15
		0.53	1.76 ± 0.18	0.90	3.31 ± 1.1	1.3	63.2 ± 17
		0.50	1.54 ± 0.16				
31	0.40	1.2	1.24 ± 0.090	1.6	1.56 ± 0.44	2.0	7.36 ± 1.4
		1.0	1.53 ± 0.078	1.4	2.21 ± 0.44	1.8	6.79 ± 0.86
		0.77	1.51 ± 0.086	1.2	3.51 ± 0.70	1.6	18.4 ± 3.0
		0.49	1.55 ± 0.17	0.89	3.24 ± 0.93	1.4	71.3 ± 16
		0.37	2.51 ± 0.32	0.77	4.33 ± 1.4	1.3	114 ± 29
		0.31	1.93 ± 0.19	0.71	4.06 ± 0.83	1.2	130 ± 27
		0.26	1.89 ± 0.23	0.67	5.09 ± 1.5	1.1	185 ± 54
45	0.40	1.7	1.19 ± 0.090	1.9	1.28 ± 0.23	2.5	3.76 ± 1.2
		1.6	1.16 ± 0.11	1.7	2.04 ± 0.45	2.4	4.43 ± 0.69
		1.3	1.40 ± 0.13	1.6	1.70 ± 0.31	2.2	6.48 ± 1.0
		1.2	1.39 ± 0.16	1.5	1.82 ± 0.30	2.0	6.73 ± 1.0
		1.0	1.40 ± 0.17	1.4	2.32 ± 0.42	1.9	9.67 ± 1.5
		0.87	1.41 ± 0.12	1.3	1.96 ± 0.30	1.7	16.4 ± 2.4
		0.64	1.47 ± 0.20	1.0	2.98 ± 0.30	1.5	28.8 ± 5.8

$\sqrt{s}$ (GeV)	p_T (GeV/c)	y_{lab}	$R(\pi^+/\pi^-)$	y_{lab}	$R(K^+/K^-)$	y_{lab}	$R(p/\bar{p})$
53	0.40	2.1	1.08 ± 0.15	2.1	1.14 ± 0.14	2.9	3.50 ± 1.0
		2.0	1.05 ± 0.13	1.9	1.98 ± 0.38	2.8	2.66 ± 0.90
		1.9	1.16 ± 0.12	1.8	1.70 ± 0.20	2.7	3.83 ± 0.90
		1.7	1.22 ± 0.051	1.7	1.85 ± 0.22	2.5	2.98 ± 0.26
		1.5	1.18 ± 0.061	1.4	2.00 ± 0.19	2.3	3.43 ± 0.38
		1.4	1.32 ± 0.13	1.2	2.27 ± 0.28	2.2	4.70 ± 0.60
		1.3	1.33 ± 0.061			1.9	6.70 ± 0.52
		1.0	1.47 ± 0.059			1.7	16.7 ± 1.6
		0.81	1.67 ± 0.078				
63	0.40	1.5	1.13 ± 0.12				
23	0.80	0.49	2.43 ± 0.25				
31	0.80	0.97	1.94 ± 0.16	1.1	2.62 ± 0.73	1.4	58.4 ± 18
		0.76	2.46 ± 0.26	0.91	3.26 ± 0.65	1.2	158 ± 45
		0.73	2.13 ± 0.19	0.87	6.39 ± 2.3	1.1	
45	0.80	1.7	1.28 ± 0.15	1.7	2.17 ± 0.32	2.1	6.19 ± 1.6
		1.5	1.51 ± 0.11	1.4	2.53 ± 0.51	1.9	10.1 ± 1.3
		1.3	1.50 ± 0.12	1.3	3.41 ± 0.56	1.7	24.9 ± 4.5
		1.1	1.66 ± 0.11	0.97	2.83 ± 0.57	1.6	40.8 ± 7.0
		0.98	1.89 ± 0.19			1.5	38.7 ± 6.2
		0.82	1.81 ± 0.13			1.4	78.8 ± 13
						1.2	112 ± 24
53	0.80	2.0	1.17 ± 0.12	2.1	2.71 ± 0.70	2.4	4.03 ± 0.74
		1.8	0.943 ± 0.089	1.9	1.98 ± 0.43	2.2	5.69 ± 0.91
		1.7	1.42 ± 0.091	1.8	1.92 ± 0.26	2.1	6.68 ± 0.69
		1.6	1.32 ± 0.12	1.7	2.54 ± 0.56	2.0	8.86 ± 1.5
		1.5	1.50 ± 0.11	1.6	2.07 ± 0.36	1.9	13.7 ± 2.3
		1.3	1.53 ± 0.15	1.5	2.64 ± 0.50	1.7	18.6 ± 2.9
		1.1	1.46 ± 0.11	1.3	3.32 ± 0.80	1.5	36.9 ± 4.4
		0.99	1.75 ± 0.11	1.1	2.89 ± 0.41	1.4	59.2 ± 6.8
63	0.80	1.5	1.25 ± 0.12			1.9	8.38 ± 0.90
45	1.2	1.4	1.59 ± 0.19	1.4	2.69 ± 0.82	1.6	47.4 ± 15
		1.1	1.68 ± 0.14	1.2	5.17 ± 1.2	1.4	135 ± 43
53	1.2	1.7	1.35 ± 0.12	1.7	2.92 ± 0.62	1.9	18.0 ± 3.8
		1.5	1.64 ± 0.15	1.6	3.52 ± 0.80	1.7	27.6 ± 5.6
		1.4	1.60 ± 0.14	1.5	4.36 ± 0.84	1.6	34.1 ± 5.6
		1.3	1.67 ± 0.16	1.4	2.86 ± 0.35	1.5	61.8 ± 12
				1.3	6.74 ± 1.5		

Table 3

Particle-to-antiparticle ratios versus y_{lab} at fixed values of p_t
(Figs. 12.1 and 12.2)

$\sqrt{s}$ (GeV)	p_T (GeV/c)	y_{lab}	$R(K^+/\pi^+)$	$R(p/\pi^+)$	$R(K^-/\pi^-)$	$R(\bar{p}/\pi^-)$
23	0.40	0.90	0.090 ± 0.013		0.0442 ± 0.010	
31	0.40	1.17	0.137 ± 0.015	0.678 ± 0.062	0.0484 ± 0.0080	0.0053 ± 0.00063
		0.99	0.0620 ± 0.015		0.0282 ± 0.0050	
		0.77	0.0718 ± 0.015		0.0251 ± 0.0060	
45	0.40	1.71	0.130 ± 0.020	0.262 ± 0.020	0.0763 ± 0.010	0.0191 ± 0.0036
		1.55	0.101 ± 0.010	0.308 ± 0.030	0.0668 ± 0.0080	0.0125 ± 0.0030
		1.33	0.102 ± 0.015		0.0617 ± 0.0080	
		1.19	0.0764 ± 0.010		0.0524 ± 0.0070	
		1.03	0.0600 ± 0.010		0.0282 ± 0.0060	
53	0.40	2.13	0.104 ± 0.010	0.187 ± 0.028	0.0990 ± 0.010	0.0422 ± 0.0040
		1.99	0.0975 ± 0.020			
		1.87	0.143 ± 0.015	0.211 ± 0.025	0.084 ± 0.0090	0.0357 ± 0.0040
		1.71	0.107 ± 0.010		0.0738 ± 0.0070	0.0201 ± 0.0020
		1.63		0.258 ± 0.026		
		1.49	0.0885 ± 0.0090		0.0522 ± 0.0050	
		1.35	0.0810 ± 0.0090			
		1.31	0.0835 ± 0.0080		0.0491 ± 0.0040	

Table 4

Particle-to-pion of the same charge ratios versus y_{lab} at p_t = 0.4 GeV/c (Fig. 12.2)

$\sqrt{s}$ (GeV)	y_{lab}	p_T (GeV/c)	$R(\pi^+/\pi^-)$	p_T (GeV/c)	$R(K^+/K^-)$	p_T (GeV/c)	$R(p/\bar{p})$
23	0.50	0.21	1.57 ± 0.14				
		0.42	1.54 ± 0.17				
		0.84	2.41 ± 0.25				
31	0.50	0.22	1.61 ± 0.11				
		0.43	1.55 ± 0.17				
23	1.0	0.36	1.42 ± 0.20	0.42	3.30 ± 0.98		
		0.42	1.84 ± 0.27				
31	1.0	0.21	1.43 ± 0.13	0.43	3.25 ± 0.53		
		0.37	1.55 ± 0.19	0.73	4.50 ± 1.3		
		0.42	1.53 ± 0.078	0.84	5.08 ± 1.9		
		0.84	1.93 ± 0.16				
45	1.0	0.22	1.37 ± 0.085	0.44	2.98 ± 0.74		
		0.38	1.54 ± 0.15	0.75	3.84 ± 0.70		
		0.43	1.41 ± 0.15				
		0.75	1.87 ± 0.16				
		0.85	1.89 ± 0.20				
53	1.0	0.22	1.58 ± 0.12	0.76	3.45 ± 0.59		
		0.38	1.53 ± 0.088				
		0.43	1.47 ± 0.11				
		0.76	1.89 ± 0.18				
		0.86	1.75 ± 0.11				
23	1.5					0.41	61.5 ± 16
31	1.5	0.62	1.12 ± 0.13	0.21	1.61 ± 0.34	0.42	44.9 ± 12
				0.41	1.89 ± 0.44		
				0.61	1.83 ± 0.75		
45	1.5	0.31	1.15 ± 0.14	0.21	2.20 ± 0.38	0.75	89.0 ± 14
		0.42	1.29 ± 0.12	0.32	2.27 ± 0.38	0.84	52.3 ± 8.5
		0.58	1.27 ± 0.10	0.37	1.73 ± 0.29	0.97	63.3 ± 14
		0.63	1.23 ± 0.14	0.42	1.94 ± 0.36	1.05	78.9 ± 19
		0.68	1.36 ± 0.12	0.48	1.88 ± 0.39	1.12	74.7 ± 15
		0.73	1.22 ± 0.11	0.52	2.18 ± 0.53	1.24	47.4 ± 14
		0.83	1.51 ± 0.11	0.57	1.92 ± 0.43		
		1.25	1.59 ± 0.19	0.63	2.29 ± 0.44		
				0.70	2.39 ± 0.45		
				0.84	2.54 ± 0.50		
				1.25	2.71 ± 0.83		

Table 7

Particle-to-antiparticle ratios versus p_t at fixed values of y_{lab} (Figs. 13.3 and 13.5)

$\sqrt{s}$ (GeV)	y_{lab}	p_T (GeV/c)	$R(\pi^+/\pi^-)$	p_T (GeV/c)	$R(K^+/K^-)$	p_T (GeV/c)	$R(p/\bar{p})$
53	1.5	0.21	1.18 ± 0.075	0.38	2.00 ± 0.24	0.76	74.1 ± 12
		0.27	1.31 ± 0.071	0.43	1.99 ± 0.20	0.86	48.1 ± 6.8
		0.32	1.25 ± 0.063	0.48	1.86 ± 0.32	0.96	52.7 ± 11
		0.37	1.18 ± 0.068	0.53	2.45 ± 0.37	1.06	46.1 ± 8.2
		0.42	1.27 ± 0.064	0.56	1.65 ± 0.29	1.16	51.8 ± 11
		0.56	1.47 ± 0.090	0.58	2.10 ± 0.38	1.26	47.9 ± 9.4
		0.58	1.59 ± 0.12	0.63	1.91 ± 0.29		
		0.63	1.49 ± 0.096	0.70	2.54 ± 0.50		
		0.68	1.48 ± 0.13	0.84	3.02 ± 0.61		
		0.71	1.44 ± 0.098	0.98	2.42 ± 0.59		
		0.73	1.31 ± 0.14	1.06	3.04 ± 0.62		
		0.78	1.21 ± 0.11	1.16	3.27 ± 0.70		
		0.84	1.43 ± 0.11	1.26	4.38 ± 1.0		
		0.98	1.64 ± 0.16	1.36	3.44 ± 0.85		
		1.16	1.55 ± 0.14	1.46	3.76 ± 1.3		
		1.26	1.56 ± 0.14				
		1.36	1.60 ± 0.19				
		1.46	1.35 ± 0.18				
63	1.5	0.22	1.64 ± 0.17				
		0.42	1.13 ± 0.14				
		0.84	1.25 ± 0.099				
31	2.0					0.19	7.13 ± 1.1
						0.30	10.6 ± 1.4
						0.35	15.4 ± 2.9
						0.39	7.38 ± 1.4
						0.40	6.78 ± 0.84
						0.60	8.63 ± 1.8
45	2.0			0.41	1.27 ± 0.27	0.20	5.27 ± 0.84
						0.32	6.64 ± 0.97
						0.36	7.63 ± 1.1
						0.40	6.48 ± 1.0
						0.41	7.67 ± 1.1
						0.47	9.99 ± 1.6
						0.51	9.29 ± 1.6
						0.56	10.5 ± 2.0
						0.61	7.77 ± 1.4
						0.66	12.8 ± 2.8
						0.71	8.17 ± 1.5
						0.82	8.18 ± 1.5
53	2.0	0.41	1.09 ± 0.13	0.21	1.96 ± 0.41	0.37	8.46 ± 0.85
		0.47	1.15 ± 0.077	0.26	1.49 ± 0.31	0.42	5.80 ± 0.49
		0.52	0.99 ± 0.093	0.31	1.40 ± 0.26	0.47	7.00 ± 0.87
		0.56	1.12 ± 0.079	0.36	1.40 ± 0.33	0.52	8.68 ± 0.95
		0.61	1.20 ± 0.083	0.41	1.55 ± 0.23	0.57	8.98 ± 1.2
		0.82	1.17 ± 0.12	0.46	2.34 ± 0.63	0.62	6.94 ± 0.80
		0.83	0.94 ± 0.090	0.82	2.34 ± 0.58	0.67	6.50 ± 0.99
		0.93	1.47 ± 0.17	0.83	1.92 ± 0.27	0.71	8.54 ± 1.2
				0.93	2.21 ± 0.48	0.77	6.01 ± 0.91
						0.82	9.74 ± 1.6
						0.92	6.36 ± 1.1
63	2.0					0.84	8.36 ± 1.1
45	2.5					0.19	4.61 ± 0.78
						0.26	4.00 ± 0.70
						0.39	4.42 ± 0.69
53	2.5					0.19	3.81 ± 0.58
						0.20	4.03 ± 0.60
						0.24	3.34 ± 0.49
						0.29	2.91 ± 0.38
						0.34	3.18 ± 0.48
						0.39	2.99 ± 0.26
						0.40	3.41 ± 0.38
						0.44	3.44 ± 0.61
						0.49	2.70 ± 0.50
						0.54	3.06 ± 0.52
						0.59	3.83 ± 0.60
						0.81	4.02 ± 0.73

Table 7 (cont.)

$\sqrt{s}$ (GeV)	y_{lab}	p_T (GeV/c)	$R(K^+/\pi^+)$	$R(p/\pi^+)$	$R(K^-/\pi^-)$	$R(\bar{p}/\pi^-)$
23	1.0	0.42	0.0918 ± 0.014		0.0513 ± 0.0073	
31	1.0	0.42	0.0593 ± 0.012			
		0.84	0.116 ± 0.019	2.08 ± 0.20	0.0279 ± 0.0040	
		1.26	0.285 ± 0.13	5.89 ± 1.2	0.0492 ± 0.012	
45	1.0	0.43	0.0672 ± 0.010		0.0316 ± 0.0062	
		0.75	0.182 ± 0.040		0.0889 ± 0.016	
		0.85	0.093 ± 0.015		0.0620 ± 0.010	
53	1.0	0.76	0.171 ± 0.030		0.0976 ± 0.015	
31	1.5	0.62			0.0834 ± 0.017	
45	1.5	0.31	0.0634 ± 0.011		0.0322 ± 0.0060	
		0.42	0.0990 ± 0.012	0.275 ± 0.030	0.0658 ± 0.0075	0.0122 ± 0.0030
		0.58	0.104 ± 0.020		0.0867 ± 0.015	
		0.63	0.154 ± 0.025		0.0700 ± 0.010	
		0.83	0.155 ± 0.025	1.01 ± 0.10	0.0918 ± 0.015	0.0386 ± 0.0061
		1.25	0.264 ± 0.055	1.94 ± 0.20		0.0700 ± 0.010
53	1.5	0.32	0.0608 ± 0.0070			
		0.37	0.0823 ± 0.0083		0.0483 ± 0.0050	
		0.42	0.084 ± 0.0080		0.0553 ± 0.0060	
		0.56	0.141 ± 0.021			
		0.58	0.142 ± 0.022		0.109 ± 0.013	
		0.63	0.163 ± 0.025	0.520 ± 0.050		
		0.71	0.186 ± 0.025		0.106 ± 0.020	
		0.84	0.201 ± 0.022	1.09 ± 0.11	0.105 ± 0.012	0.0434 ± 0.0060
		0.98	0.270 ± 0.055	1.64 ± 0.17	0.182 ± 0.036	0.0615 ± 0.014
		1.13	0.309 ± 0.050	1.62 ± 0.16		
		1.16	0.358 ± 0.070	1.91 ± 0.19	0.169 ± 0.025	0.0553 ± 0.010
		1.25	0.331 ± 0.050		0.154 ± 0.025	
		1.26	0.401 ± 0.060	1.84 ± 0.18	0.148 ± 0.020	0.0678 ± 0.015
		1.27	0.363 ± 0.050	2.36 ± 0.24	0.123 ± 0.015	
		1.36	0.400 ± 0.10		0.186 ± 0.020	
		1.46	0.416 ± 0.10		0.419 ± 0.040	
53	2.0	0.41	0.108 ± 0.012	0.174 ± 0.020	0.0908 ± 0.010	0.0422 ± 0.0025
		0.47			0.101 ± 0.020	0.051 ± 0.0051
		0.51	0.0888 ± 0.020			
		0.52		0.405 ± 0.042		0.0465 ± 0.0050
		0.56		0.346 ± 0.035		0.0588 ± 0.0060
		0.61	0.221 ± 0.035			0.0642 ± 0.0070
		0.62		0.336 ± 0.034		
		0.72	0.165 ± 0.025	0.424 ± 0.042		
		0.82	0.257 ± 0.035	0.444 ± 0.045	0.136 ± 0.015	0.0738 ± 0.0080
		0.83	0.246 ± 0.035		0.121 ± 0.015	0.0637 ± 0.010
		0.93	0.262 ± 0.040	0.565 ± 0.053	0.175 ± 0.020	0.130 ± 0.030

Table 8

Particle-to-pion of the same charge ratios versus p_t at fixed values of y_{lab} (Figs. 13.4 and 13.5)